The role of aneuploidy in the evolution of cancer drug resistance

Remus Stana[1], Uri Ben-David[2], Daniel B. Weissman[3], and Yoav Ram[1,*]

[1]School of Zoology, Faculty of Life Sciences, Tel Aviv University, Tel Aviv, Israel
[2]Department of Human Molecular Genetics and Biochemistry, Faculty of Medicine, Tel Aviv University, Tel Aviv, Israel
[3]Department of Physics, Emory University, Atlanta, GA
[*]Corresponding author: Yoav Ram (e-mail: yoavram@tauex.tau.ac.il)

May 15, 2024

Abstract

Evolutionary rescue is the process by which a population survives a sudden environmental change that initially causes the population to decline towards extinction. A prime example of evolutionary rescue is the ability of cancer to survive exposure to treatment. One evolutionary mechanism by which a population of cancer cells can adapt to chemotherapy is aneuploidy. Aneuploid cancer cells can have higher fitness in an environment altered by anti-cancer drugs, e.g., because of incomplete pathways targeted by the drugs. Indeed, aneuploidy is highly prevalent in tumors, and moreover, some anti-cancer drugs fight cancer by increasing chromosomal instability. Here, we examine how aneuploidy impacts the fate of a population of cancer cells. We use multi-type branching processes to approximate the probability that a tumor survives drug treatment as a function of the initial tumor size, the rates at which aneuploidy and other beneficial mutations occur, and the growth rates of the sensitive and resistant cells. Additionally, we investigate the effect on the probability of evolutionary rescue of having a fraction of aneuploid tumor cells before the onset of therapy. We also approximate the mean recurrence time for the tumor to revert back to its initial size following treatment. We find that aneuploidy can play an important role in the relapse of smaller secondary tumors who have not yet been detected.

Keywords: whole-chromosome duplication, evolutionary model, adaptive evolution, cancer, drug resistance, chromosome instability

Introduction

Aneuploidy in cancer. Each year approximately 10 million people die from cancer (Kocarnik et al., 2022), so understanding the factors that contribute to failure of interventions is of great importance. One hypothesized factor is aneuploidy, where cells are characterized by an imbalanced karyotype and chromosome copy number alterations (Schukken and Foijer, 2018). Aneuploidy is caused by chromosomal instability, the mitotic process in which cells suffer from chromosome mis-segregation. Importantly, aberrations in chromosome copy number allow cancer cells to survive under stressful conditions such as drug therapy (Lukow et al., 2021, Rutledge et al., 2016). Indeed, cancer cells are often aneuploid and aneuploidy is associated with poor patient outcomes (Ben-David and Amon, 2020, Smith and Sheltzer, 2018).

Ippolito et al. (2021) induced aneuploidy in cancer cell lines by exposing them to reversine, a small-molecule inhibitor of the mitotic kinase Mpsi1 and then to chemotherapeutic agents such as vemurafenib. Reversine-treated cells had higher proliferation rate in the environment altered by anti-cancer drugs compared to wildtype cancer cells. Similarly, Lukow et al. (2021) induced aneuploidy in cancer cells and observed that such cells have an advantage compared to wildtype cells during chemotherapy, despite having lower fitness before the onset of chemotherapy. One proposed mechanism through which aneuploidy is able to confer resistance to chemotherapeutics is by antagonizing cell division, which prevents the drugs from damaging DNA and microtubules (Replogle et al., 2020).

An important aspect of aneuploidy is the rate with which cells become aneuploid, which is several orders of magnitude higher than the beneficial mutation rate (Bakker et al., 2023). Consequently, a cell exposed to a stress such as chemotherapeutic drugs can acquire aneuploidy faster compared to acquiring a mutation. Morover several proposed anti-cancer drugs elevate the rate of mis-segregation in order to fight cancer cells (Lee et al., 2016).

Evolutionary rescue. Populations adapted to a certain environment are vulnerable to environmental changes, which might cause extinction of the population. Examples of such environmental changes include climate change, invasive species, and the onset of drug therapies. Adaptation is a race against time as the population size decreases in the new environment (Tanaka and Wahl, 2022). *Evolutionary rescue* is the process where the population acquires a trait that increases fitness in the new environment such that extinction is averted. It is mathematically equivalent to the problem of crossing of fitness valley (Weissman et al., 2009, 2010). There are three potential ways for a population to survive environmental change: migration to a new habitat similar to the one before the onset of environmental change (Cobbold and Stana, 2020, Harsch et al., 2014, Zhou, 2022); adaptation by phenotypic plasticity without genetic modification (Carja and Plotkin, 2017, 2019, Gunnarsson et al., 2020, Levien et al., 2021); and adaptation through genetic modifications, e.g., mutation (Gomulkiewicz and Holt, 1995, Orr and Unckless, 2014, Uecker and Hermisson, 2011, 2016, Uecker et al., 2014).

Gunnarsson et al. (2020) analyzed a model where a tumor consisting of two populations of cancer cells, one drug resistant and the other drug sensitive, is able to evade extinction by cells switching between the two phenotypes through epigenetic mutations. They found that even when the drug resistant type is barely viable the epimutations have the effect of guaranteeing evolutionary rescue. Evolutionary rescue in one step where an initially declining population, after a sudden environmental change, has to acquire a mutation in order to survive extinction has been studied by Orr and Unckless (2008, 2014). They analyzed a model where the mutant strain is present in small numbers at the onset of therapy and concluded that this can significantly enhance the probability that the population will survive.

Most models focus on the probability that at most one mutation rescues the population. How multiple mutations contribute to the survival of the population is less explored, but Wilson et al. (2017) have shown that evolutionary rescue is significantly enhanced by soft selective sweeps when

multiple mutations contribute towards evolutionary rescue. Evolutionary rescue that requires two successive mutations (i.e., two steps) has been investigated using diffusion approximation by Martin et al. (2013) who tested the predictions of their model with data from experiments with yeast and bacteria.

Here we study evolutionary rescue after a sudden environment change caused by the initiation of chemotherapy. We estimate the effect of aneuploidy on the probability of evolutionary rescue when it acts as an evolutionary stepping stone towards resistant cancer cells. We also estimate the mean time until a tumor cell population reaches its pre-treatment size following drug therapy. Given that aneuploidy is present in many tumors even before the onset of therapy (Lukow et al., 2021), we also consider the effect of pre-treatment standing genetic variation on the evolutionary dynamics. Additionally, we are interested in the timescale of evolutionary rescue and the effect that aneuploidy has on the time necessary for the tumor to overcome drug therapy.

Methods

Evolutionary model. We follow the number of cancer cells that have one of three different genotypes at time t: wildtype, w_t; aneuploid, a_t; and mutant, m_t. These cells divide and die with rates λ_k and μ_k (for $k = w, a, m$). The difference between the division and death rate is $\Delta_k = \lambda_k - \mu_k$. We assume the population of cells is under a strong stress, such as drug therapy, to which the wildtype genotype is susceptible or sensitive and therefore $\Delta_w < 0$, whereas the mutant is resistant to the stress, $\Delta_m > 0$. We analyze three scenarios: in the first, aneuploid cells are partially resistant, $\Delta_m > \Delta_a > 0$; in the second, aneuploid cells are tolerant, $0 > \Delta_a > \Delta_w$ (see Brauner et al., 2016, for the distinction between susceptible, resistant, and tolerant); in the third, aneuploid cells are non-growing, stationary, or growing or dying only very slowly, that is, either slightly tolerant or slightly resistant, such that $\Delta_a \approx 0$, in a sense that we will make precise below. We assume that both chromosomal missegregation and mutation occur during the process of mitosis. Wildtype cells may divide and then missegregate to become aneuploids at rate $u\lambda_w$. Both aneuploid and wildtype cells may divide and mutate to become mutants at rates $v\lambda_a$ and $v\lambda_w$, respectively. To model standing genetic variation, we assume that before the onset of therapy, wildtype cells become aneuploid with rate $\tilde{u}\lambda_w$ (which may differ from $u\lambda_w$) and that aneuploidy confers a fitness cost s in the drug-free environment, that is, we assume that aneuploid cells have an increased death rate compared to wildtype cells in a drug-free environment. See Figure 1 for a schematic representation of the model and Figure 2 for sample trajectories of the different genotypes.

Stochastic simulations. Simulations are performed using the *Gillespie stochastic simulation algorithm* (Gillespie, 1976, 1977) implemented in Python (Van Rossum and Others, 2007). The simulation monitors the number of cells of each type: wildtype, aneuploid, and mutant. The wildtype population initially consists of $w_0 = N$ cells, whereas the other cell types are initially absent.

The cell population at time t is represented by the triplet (w_t, a_t, m_t). The following describes the events that may occur (right column), the rates at which they occur (middle column), and the effect these events have on the population (left column, see Figure 1):

$$
\begin{aligned}
(+1,0,0): &\quad \lambda_w w_t\,(1-u-v) \quad \big(\text{birth of wildtype cell}\big),\\
(-1,0,0): &\quad \mu_w w_t \quad \big(\text{death of wildtype cell}\big),\\
(0,+1,0): &\quad u\lambda_w w_t \quad \big(\text{wildtype cell divides and becomes aneuploid}\big),\\
(0,0,+1): &\quad v\lambda_w w_t \quad \big(\text{wildtype cell divides and becomes mutant}\big),\\
(0,+1,0): &\quad \lambda_a a_t\,(1-v) \quad \big(\text{birth of aneuploid cell}\big),\\
(0,-1,0): &\quad \mu_a a_t \quad \big(\text{death of aneuploid cell}\big),
\end{aligned}
$$

$$
\begin{aligned}
(0,0,+1): &\quad \nu\lambda_a a_t \quad \left(\text{aneuploid cell divides and becomes mutant}\right),\\
(0,0,+1): &\quad \lambda_m m_t \quad \text{(birth of mutant cell)},\\
(0,0,-1): &\quad \mu_m m_t \quad \text{(death of mutant cell)}.
\end{aligned}
$$

For the remaining of this paper we assume that the division rates for wildtype and aneuploid cells can be written as $\lambda_w w_t\,(1-u-v) \approx \lambda_w w_t$ and $\lambda_a a_t\,(1-v) \approx \lambda_a a_t$ because $u, v \ll 1$ (Table 1). Each iteration of the simulation loop starts with computing the rates ν_k of each event k. We then draw the time until the next event, Δt, from an exponential distribution whose rate parameter is the sum of the rates of all events, such that $\Delta t \sim \text{Exp}(\sum_j \nu_j)$. Then, we randomly determine which event occurred, where the probability for event k is $p_k = \nu_k / \sum_j \nu_j$. Finally, we update the number of cells of each type according to the event that occurred and update the time from t to $t + \Delta t$. We repeat these iterations until either the population becomes extinct (the number of cells of all types is zero) or the number of mutant cells is high enough so that its extinction probability is $< 0.1\%$, that is until

$$
m_t > \left\lfloor \frac{3\log 10}{\log\left(\lambda_m/\mu_m\right)} \right\rfloor + 1,
$$

which we obtain by solving $1-(1-p_m)^{m_t} = 0.999$ for m_t with $p_m = \Delta_m/\lambda_m$ as the probability that a single mutant escapes stochastic extinction (see Appendix A).

When simulations are slow (e.g., due to large population size), we use τ-leaping (Gillespie, 2001), where we assume that the change in the number of cells of genotype k in a fixed time interval Δt is Poisson distributed with mean $\nu_k \Delta t$. If the change in the number of cells is negative and larger than the subpopulation size then the subpopulation size is updated to be zero.

Parameterization. To parametrize the simulations, we assume that the cells under consideration are melanoma cells and rely on Rew and Wilson (2000) and Bozic et al. (2013) for the division and death rates, respectively. Rew and Wilson (2000) report *in vivo* measurements of the potential doubling times (the waiting time for the number of cells in the tumor to double disregarding cell death) for a large set of cancer types. The division rate is obtained as $\lambda = \log 2/T \approx 0.1$ per day. We select this to be the division rate for wildtype and mutant cells.

Bozic et al. (2013) report the growth rate Δ_w for wildtype melanoma cancer cells from which they deduce the death rate $0.11 \leq \mu_w \leq 0.17$. We use $\mu_w = 0.14$ per day. Additionally, they observe the growth rate of cancer cells prior to treatment to be 0.01, which we use as the growth rate of mutant cells, which are resistant to the drug. Thus, we use $\mu_m = 0.1 - 0.01 = 0.09$ per day as the death rate for mutant cells.

Aneuploid death rate μ_a is set to the same value as the mutant death rates, $\mu_m = 0.09$ per day, given that aneuploidy increases resistance to the drug, such as cisplatin, by antagonizing cell division (Replogle et al., 2020). Aneuploid division rate is selected such that the aneuploid growth rate $\Delta_w \ll \Delta_a \ll \Delta_m$ which means that $0.06 \leq \lambda_a \leq 0.1$. For most of our simulations we use $\lambda_a = 0.0899$ per day, such that aneuploidy can only act as a *stepping stone* for the generation of the mutant that rescues the cancer cell population.

We assume the mutation rate is 10^{-7} per gene per cell division (Loeb, 2001) and since we assume that a single target gene confers resistance to the drug, we use $\nu = 10^{-7}$ per cell division. Bakker et al. (2023) determined that the missegregation rate must be between $10^{-3} - 10^{-2}$ per chromosome per cell division with the optimal value being 6.2×10^{-3} per chromosome per cell division (for $u \ll 10^{-3}$ no adaptation occurs and for $u \gg 10^{-2}$ cells will acquire lethal nullisomies where both pairs of chromosomes are lost). Ippolito et al. (2021) observed that trisomy in Chr II and VI are most likely to confer increased resistance against the chemotherapeutic agent vemurafenib for A375 cells. We assume that if a tumor is aneuploid then it most likely has trisomy (Gisselsson et al., 2010) in the pre-treatment environment and that cells with more than one trisomy are very unlikely to survive.

Additionally, we assume that all trisomies are equally likely and, as a result, we select $u = 10^{-2}$ per cell division. For the missegregation rate in the drug-free environment, $\tilde{u}$, we use the lower-end value of $\tilde{u} = 2 \times 10^{-3}$ per cell division, as some drugs increase the rate of aneuploidy (Mason et al., 2017, Wang et al., 2019).

The fitness cost s of aneuploidy before the onset of therapy is difficult to estimate as we are interested in a specific type of aneuploidy that improves the fitness of cancer cells in an environment altered by drugs. We derive s by using the formula $s = \tilde{u}\lambda_w/f$, where f is the fraction of aneuploid cancer cells. To estimate f, we note that Lukow et al. (2021) mixed wildtype and aneuploid A375 melanoma cells at 50 : 50 ratio, cultured them in drug-free environment and observed the ratio evolve as a function of time with the aneuploid cells declining to 15% after 24 days. We obtain the fitness cost s using the formula $s = \left|\log\left[0.15/(1-0.15)\right]/24\right| \approx 0.07$ per day (Chevin, 2011). As a result, the fraction of cancer cells with aneuploidy of interest is $f = 2 \times 10^{-3} \times 10^{-1}/0.07 = 0.28\%$ (i.e., 0.28% of pre-treatment cancer cells have the aneuploidy of interest).

We note that when we refer to wildtype cancer cells we include those cells that have any aneuploidy other than trisomy in Chr II and VI as those are the aneuploid cells that are hypothesized to have higher fitness in the environment altered by drugs such as vemurafenib.

Density-dependent growth. In our analysis, we assume that lineages produced by cells from the initial population divide and die independently of each other. However, the cells will compete for resources, but we expect that this competition can be neglected because the drug will cause the cell density to rapidly drop below the carrying capacity at which competition is most important. To test this, we simulate a logistic growth model, with division and death rates given by:

$$\begin{aligned}
\lambda'_w &= \lambda_w, \\
\mu'_w &= \mu_w, \\
\lambda'_a &= \lambda_a, \\
\mu'_a &= \mu_a + \lambda_a \frac{w+a+m}{K}, \\
\lambda'_m &= \lambda_m, \\
\mu'_m &= \mu_m + \lambda_m \frac{w+a+m}{K},
\end{aligned}$$

where K is the tumor carrying capacity. The effective carrying capacity in this model is $K_e = K\Delta_a/\lambda_a \approx 10^6$ for $K = 10^8, \lambda_a = 0.0901, \mu_a = 0.09$, where we define the effective carrying capacity to be the population size at which the aneuploid division rate is equal to the aneuploid death rate.

Code and data availability. All source code is available online at https://github.com/yoavram-lab/EvolutionaryRescue.

Results

Evolutionary rescue probability

In our model, *evolutionary rescue* occurs when resistant cells appear and establish (avoid random extinction) in the population ($m_t \gg 1$) before the population becomes extinct ($w_t = a_t = m_t = 0$). Aneuploidy may contribute to evolutionary rescue by either preventing (when $\Delta_a > 0$) or delaying (when $0 > \Delta_a > \Delta_w$) the extinction of the population before mutant cells appear and establish. We assume independence between clonal lineages starting from an initial population of N wildtype cells (we check the effect of density-dependent growth on our results below). We therefore define p_w as

the probability that a lineage starting from a single wildtype cell avoids extinction by acquiring drug resistance. Thus, $N^* = 1/p_w$ is the threshold tumor size above which evolutionary rescue is very likely, and the rescue probability is given by

$$p_{\text{rescue}} = 1 - \left(1 - p_w\right)^N \approx 1 - \mathrm{e}^{-Np_w} = 1 - e^{-N/N^*}, \tag{2}$$

where the approximation $(1-p_w) \approx e^{-p_w}$ assumes that p_w (but not necessarily Np_w) is small. Indeed, when $N < 1/p_w$, then the probability for evolutionary rescue is $p_{\text{rescue}} \approx Np_w$ and when $N > 1/p_w$, it is $p_{\text{rescue}} \approx 1$, justifying the definition of N^* as the threshold tumor size for evolutionary rescue.

We use the theory of multi-type branching processes to find approximate expressions eqs. (A4), (A7) and (A11) for p_w in different regimes (see appendix A). Substituting these into $N^* = 1/p_w$, we find approximations for the threshold tumor size, N^*. For these approximations, an important quantity is $T^* = (4v\lambda_a^2\Delta_m/\lambda_m)^{-1/2}$, which is the critical time an aneuploid lineage needs to survive to produce a resistant mutant that avoids random extinction. First, if aneuploidy is very rare ($u\lambda_a T^* < 1$), or if aneuploidy is rare ($u\lambda_a < -\Delta_a$) and very sensitive to the drug ($\Delta_a T^* < -1$), then evolutionary rescue will likely occur by a direct resistance mutation in a sensitive wildtype cell without the involvement of aneuploidy, such that

$$N_m^* \approx \frac{|\Delta_w|}{v\lambda_w}\frac{\lambda_m}{\Delta_m}. \tag{3}$$

Here, $|\Delta_w|/(v\lambda_w)$ is the ratio of the rate at which wildtype cells are decreasing in number and the rate at which they are mutating. Notably, the aneuploidy parameters (u, λ_a, μ_a) do not affect N_m^*.

Otherwise, aneuploidy is frequent enough ($u\lambda_a > \max\left(-\Delta_a, 1/T^*\right)$) to affect the evolution of drug resistance. The threshold tumor size can then be approximated by one of the following scenarios, depending on $\Delta_a T^*$, the change in the aneuploid log-population size during the critical time,

$$N_a^* \approx \frac{|\Delta_w|}{u\lambda_w} \cdot \begin{cases} \frac{|\Delta_a|}{v\lambda_a}\frac{\lambda_m}{\Delta_m}, & \Delta_a T^* \ll -1 \text{ (tolerant aneuploids)}, \\ 2\lambda_a T^*, & -1 \ll \Delta_a T^* \ll 1 \text{ (stationary aneuploids)}, \\ \frac{\lambda_a}{\Delta_a}, & \Delta_a T^* \gg 1 \text{ (resistant aneuploids)}. \end{cases} \tag{4}$$

These approximations perform very well when compared to results of stochastic evolutionary simulations (Figures 3 and 4). The first line describes the scenario in which aneuploid cells are still effectively killed by the treatment, but not as quickly as the wildtype. In the second scenario, aneuploid cells are sufficiently resistant that the expected size of each aneuploid lineage is roughly 1. In both of these scenarios, aneuploidy increases the probability of rescue by slowing or halting the decrease of the tumor population size, allowing more opportunities for producing resistant mutants. In the third scenario, aneuploid cells are sufficiently resistant for the population to re-grow the tumor even without additional resistance mutations. Notably, in this scenario the mutant parameters (v, λ_m, and Δ_m) do not affect N_a^* beyond their effect on T^*. In all scenarios, N_a^* is proportional to $1/u$ such that increasing the missegregation rate u will decrease the threshold tumor size (Figure 4B). Furthermore, increasing the aneuploid growth rate Δ_a (which appears both in the terms and in the conditions), also reduces the threshold tumor size, with a sharp decrease around $\Delta_a = 0$, but the effect is minor when $|\Delta_a|$ is small compared to T^* as this would result in the second scenario where $dN_a^*/d\Delta_a = 0$ (Figure 4A).

Using eqs. (3) and (4), we can find the ratio of threshold tumor size for rescue via aneuploidy (u is high) or via direct mutation (u is low),

$$\frac{N_a^*}{N_m^*} \approx \begin{cases} \frac{|\Delta_a|}{u\lambda_a}, & \Delta_a T^* \ll -1, \\ \frac{1}{u}\left(v\frac{\Delta_m}{\lambda_m}\right)^{1/2}, & -1 \ll \Delta_a T^* \ll 1, \\ v\frac{\Delta_m}{\lambda_m}\left(u\frac{\Delta_a}{\lambda_a}\right)^{-1}, & \Delta_a T^* \gg 1. \end{cases} \tag{5}$$

As expected, this ratio increases with the mutation rate v and decreases with the aneuploidy rate u. In the first scenario, $|\Delta_a|/(u\lambda_a)$ is the ratio of the expected time for an aneuploid lineage to appear, $1/(u\lambda_a)$, and the expected time until that lineage disappears, $1/|\Delta_a|$. In the third scenario, $\left(v\frac{\Delta_m}{\lambda_m}\right)/\left(u\frac{\Delta_a}{\lambda_a}\right)$ is the ratio of the rates of formation of resistant mutants that avoid extinction and partially resistant aneuploids that avoid extinction. In the second scenario, $\frac{1}{u}\left(v\frac{\Delta_m}{\lambda_m}\right)^{1/2} = \sqrt{\frac{\Delta_a}{u\lambda_a}v\frac{\Delta_m}{\lambda_m}\left(u\frac{\Delta_a}{\lambda_a}\right)^{-1}}$, which is the geometric mean of the first and third scenarios.

Interestingly, increasing both the aneuploid division rate, λ_a, and the aneuploid death rate, μ_a, such that the growth rate Δ_a remains constant, leads to decreases in T^*, pushing the system to the second scenario. In this scenario, increasing the division rate λ_a should also increase the mutation rate $v\lambda_a$ in aneuploid cells, as mutations mostly occur during division, so overall the threshold tumor size N_a^* is unaffected by the division rate λ_a (i.e., $d\lambda_a T^*/d\lambda_a = 0$). Thus, if aneuploid cells rapidly die due to the drug but compensate by rapidly dividing, further increasing the division rate will *not* facilitate adaptation. This is consistent with experimental findings where aneuploidy confers resistance by decreasing the division rate (Replogle et al., 2020).

We can categorize tumors by their size: small tumors with size $N < N_a^*$ that are unlikely to survive treatment, intermediate tumors with size $N_a^* < N < N_m^*$ that rely on aneuploidy for evolutionary rescue, and large tumors with size $N > N_m^*$ that could overcome the effect of drug treatment even without aneuploidy. For the parameter values in Table 1 with $\lambda_a = 0.0899, \mu_w = 0.14, u = 10^{-2}, v = 10^{-7}$, we are in the tolerant aneuploid scenario, and substituting in eqs. (3) and (4), we have $N_a^* \approx 4 \times 10^6$ and $N_m^* \approx 4 \times 10^7$. Hence, we obtain the ratio $N_a^*/N_m^* \approx 0.11$ (eq. (5)), that is, aneuploidy reduces the threshold tumor size by approximately 89%. Interestingly, the threshold between small and intermediate tumors, N_a^*, is similar to the tumor detection threshold of 4×10^6 cells for a wide variety of tumors as reported by Avanzini and Antal (2019).

Density-dependent growth. In our analysis we used branching processes, which assume that growth (division and death) is density-independent. However, growth may be limited by resources (oxygen, nutrients, etc.) and therefore depend on cell density. We therefore performed stochastic simulations of a logistic growth model with a carrying capacity (see Methods). We find that our density-independent approximations agree with results of simulations with density-dependent growth for biologically relevant parameter values (Figure S1).

Standing vs. *de-novo* genetic variation. In the above we assumed that at the onset of drug treatment, the initial tumor consisted entirely of wildtype cells that are drug sensitive. However, aneuploidy is likely produced even before the onset of treatment at some rate $\tilde{u}$ and confers a deleterious fitness effect s in the absence of the drug (Giam and Rancati, 2015, Replogle et al., 2020). Furthermore, the aneuploidy rate in the presence of drugs is likely higher than in their absence, $\tilde{u} < u$ (Mason et al., 2017, Wang et al., 2019). But if the number of cells in the tumor N is large (as expected if the tumor is treated with a drug), there may already be a fraction $f \approx \tilde{u}\lambda_w/s$ of aneuploid cells in the population (here we assume that the drug affects the wildtype death rate but not the division rate and therefore we use λ_w for the wildtype division rate in the drug-free environment).

Therefore, the threshold tumor size with standing generation variation, $\tilde{N}_a^*$, is similar to the threshold with de-novo variation, N_a^*, except that the sensitive growth rate $|\Delta_w|$ is replaced with the aneuploidy cost s, such that

$$\frac{\tilde{N}_a^*}{N_a^*} = \frac{u}{\tilde{u}}\frac{s}{|\Delta_w|}. \tag{6}$$

Comparing this approximation of $\tilde{N}_a^*/N_a^*$ to results of stochastic simulations, we find that the approximations perform very well (Figure 5). Standing genetic variation will drive evolutionary rescue if wildtype cells die rapidly (growth rate Δ_w is very negative) due to a strong effect of the drug on

sensitive cells, or if the aneuploidy cost in the drug-free environment, s, is small. In contrast, *de-novo* aneuploid cells will have a greater contribution to rescue if the aneuploidy cost s is large, the effect of the drug on sensitive cells is weak (Δ_w is close to zero), or if the drug induces the appearance of aneuploid cells ($u > \tilde{u}$). For example, with $\lambda_w = 0.1, \mu_w = 0.14, u = 10^{-2}, \tilde{u} = 2 \times 10^{-3}, s = 0.07$, the ratio of the threshold tumor sizes for standing vs. *de-novo* variation is $\tilde{N}_a^*/N_a^* \approx 8.75$, which means that *de-novo* genetic variation is the main driver of evolutionary rescue.

Using eqs. (3), (4) and (6), we can find the ratio of threshold tumor size for rescue via standing genetic variation to the threshold for rescue via direct mutation,

$$\frac{\tilde{N}_a^*}{N_m^*} = \frac{\tilde{N}_a^*}{N_a^*}\frac{N_a^*}{N_m^*} \approx \frac{s}{|\Delta_w|} \begin{cases} \frac{|\Delta_a|}{\tilde{u}\lambda_a}, & \Delta_a T^* \ll -1, \\ \frac{1}{\tilde{u}}\left(v\frac{\Delta_m}{\lambda_m}\right)^{1/2}, & -1 \ll \Delta_a T^* \ll 1, \\ v\frac{\Delta_m}{\lambda_m}\left(\tilde{u}\frac{\Delta_a}{\lambda_a}\right)^{-1}, & \Delta_a T^* \gg 1. \end{cases} \tag{7}$$

Evolutionary rescue through direct mutation is more likely if the cost of aneuploidy s is very large or the effect of the drug Δ_w is small. In contrast, standing genetic variation will drive adaptation if the pre-treatment chromosome missegreagation rate $\tilde{u}$ is very large. The ratio does not depend on the rate of chromosome missegregation induced by the drug u. However, if the aneuploid growth rate Δ_a increases, then evolutionary rescue is driven by standing genetic variation. For the parameter values of $\lambda_w = 0.1, \lambda_a = 0.0899, \lambda_m = 0.1, \mu_w = 0.14, \mu_a = 0.09, \mu_m = 0.09, \tilde{u} = 10^{-3}, v = 10^{-7}$, we are in the tolerant aneuploid scenario and obtain the ratio $\tilde{N}_a^*/N_m^* \approx 0.9625$, which means that standing genetic variation reduces the threshold tumor size by approximately 4‰. Therefore, standing genetic variation does not drive evolution of drug resistance when compared to *de-novo* aneuploidy, but it does offer a slight advantage when compared with direct mutation.

Recurrence time due to evolutionary rescue

When evolutionary rescue occurs, the time until recurrence of the tumor may still be very long. We therefore explored the time until recurrence of the tumor, that is, the time until the tumor reaches its original size, N. When the expected number of resistant lineages that avoid extinction is small, the expected recurrence time can be estimated by adding two terms: the *mean evolutionary rescue time*, which is the waiting time for appearance of a resistant lineage that avoids extinction (conditioned on such an event occurring in the first place), and the *mean proliferation time*, which is the expected time for that lineage to grow to N cells. However, when the expected number of resistant lineages is large, the dynamics of the number of mutant cells is deterministic (i.e., it can be modeled by a system of ODEs, eq. (D2)) and the mean recurrence time cannot be separated into the mean evolutionary rescue time and mean proliferation time because multiple mutant lineages contribute towards the mutant population size reaching the initial tumor size. Of particular interest is the distribution of the evolutionary rescue time and recurrence time with tolerant aneuploid cells ($\Delta_a T^* \ll 1$), for which we focus on the parameter values $\lambda_w = 0.1, \lambda_a = 0.0899, \lambda_m = 0.1, \mu_w = 0.14, \mu_a = 0.09, \mu_m = 0.09, u = 10^{-2}, v = 10^{-7}$.

Evolutionary rescue time. In Appendix C we have derived approximations for τ_m, the mean evolutionary rescue time without aneuploidy ($u = 0$), and τ_a, the mean rescue time with aneuploidy ($u > 0$), both conditioned on evolutionary rescue occurring. These approximations are in good agreement with simulation results for small, intermediate, and large tumor sizes (Figures S2 and S6). The mean rescue time with aneuploidy for small and large tumors follows these expressions (Appendix C),

$$\tau_a \approx \begin{cases} -\frac{1}{\Delta_w} - \frac{1}{\Delta_a}, & N \ll N_a^*, \\ \frac{1}{v\lambda_w N}\frac{\lambda_m}{\Delta_m}, & N \gg N_m^*. \end{cases} \tag{8}$$

For small tumors ($N \ll N_a^*$), the mean rescue time is a function of the wildtype and aneuploid growth rates and independent of the other model parameters, including tumor size (blue line in Figure S6). Increasing the wildtype or aneuploid growth rates leads to an increase in the mean rescue time, because the corresponding cells will survive for longer and will produce additional rescue mutations at latter times. In our focus parameter regime, we have $\Delta_w = -0.04$ and $\Delta_a = -10^{-4}$, such that the mean rescue time is mainly determined by the aneuploid growth rate, $\tau_a \approx 10^4$ days.

For large tumors ($N \gg N_m^*$), the mean evolutionary rescue time (eq. (8)) is independent of parameters characterizing aneuploid cells or their production (u, λ_a, and Δ_a). Increasing the per division mutation rate, v, leads to faster appearance of a rescue mutation and hence reduced mean rescue time. Finally, increasing the tumor size leads to shorter mean rescue time, as there are more wildtype cells that can mutate to become resistant.

Given that a fraction $f \approx 0.28\%$ of the initial cancer cell population is expected to be aneuploid even before the onset of drug treatment, we want to know whether the mean evolutionary rescue time is affected by the standing genetic variation. We calculated the mean evolutionary rescue time with standing genetic variation $\tilde{\tau}_a$ (eq. (C10)) and compared our result with simulations in Figure S9. We note that standing genetic variation does not have a significant effect on the mean evolutionary rescue time.

In Appendix E we calculated the probability that a rescue mutation has been generated by time t. This allows us to examine whether aneuploidy accelerates or delays evolutionary rescue. We find that anenploidy accelerates evolutionary rescue after $1/\Delta_a \approx 100$, days after which no more rescue mutations are generated through direct mutation (Figure 6A). This shows that rescue mutations are generated in aneuploid cells at latter timescales then in sensitive cells and, thus, aneuploidy increases the *window of opportunity* for evolutionary rescue.

Recurrence time. We next approximated the mean time for the population of mutant cancer cells to reach the initial, pre-treatment population size N, which we denote the recurrence time τ_a^r (Appendix D),

$$\tau_a^r \approx \begin{cases} -\frac{1}{\Delta_w} - \frac{1}{\Delta_a} + \frac{\log p_m N}{\Delta_m}, & N \ll N_a^*, \\ \frac{1}{\Delta_m} \log \frac{\Delta_m - \Delta_w}{v \lambda_w}, & N \gg N_m^*. \end{cases} \tag{9}$$

Figures 7 and S7 show the agreement between our approximations and simulations. For small tumors ($N \ll N_a^*$), the mean recurrence time can be approximated as the sum of the mean time for the first rescue mutation to appear and the mean time for its lineage to reach size N. The mean recurrence time grows logarithmically with tumor size N and is the same order of magnitude as the mean evolutionary rescue time. Increasing the mutant growth rate Δ_m decreases recurrence times while increasing the wildtype and aneuploid growth rates, Δ_w and Δ_a respectively, increases the recurrence time. For large tumors ($N \gg N_m^*$), the dynamics of the number of mutant cells is deterministic and the mean recurrence time becomes independent of the initial tumor size N. Increasing either the mutant growth rate Δ_m or the mutation rate v leads to a decrease in the time for the tumor to rebound to its initial size. In addition, drugs that significantly increase the wildtype death rate μ_w and do not affect the division rate λ_w delay cancer recurrence. Consequently, patients treated with such drugs may require a longer period of monitoring to guarantee the effectiveness of the treatment.

We note that, for small and large tumors, when $N \ll N_a^*$ or $N \gg N_m^*$, the asymptotic expressions for the mean recurrence time are independent of the chromosome missegregation rate u, and therefore the rate at which the drug induces aneuploidy has no effect on the time necessary for the tumor to rebound to its initial size N.

In Appendix F we derive the probability that a mutant cancer cell population has not reached size N by time t. Figure 6B shows agreement between our approximations and stochastic simulations for various values of N. Additionally, we derive the distribution of the recurrence time for the scenario $N = 10^6$ (small tumor), noting that the distribution is wide and right-skewed (Figure S4). It is highly

unlikely to observe the recurrence of tumors at times smaller then $\frac{1}{\Delta_m} \log \frac{\Delta_m - \Delta_w}{v\lambda_w} \approx 1542$ days for the parameter values $\lambda_w = 0.1, \lambda_a = 0.0899, \lambda_m = 0.1, \mu_w = 0.14, \mu_a = 0.09, \mu_m = 0.09, u = 10^{-2}, v = 10^{-7}$ and independent of initial tumor size N (Figure 6B).

The detection time τ_a^M can be defined as the time for the tumor size to reach detection threshold M. We derive the mean detection time for $M = 10^7$ in Appendix D. We observe that for small and intermediate sized tumors the effect of the detection size M on τ_a^M is negligible when compared to the scenario where the detection size is equal to the initial population size N (i.e., $\tau_a^r \approx \tau_a^M$ for $N < N_m^*$). However, for large tumors the mean recurrence time to detection size M decreases logarithmically with tumor size N while τ_a^r is constant (Figure S8). Additionally, for large tumors we have $M < N_m^* < N$ so the mean detection time is shorter for such tumors compared to the mean recurrence time, that is, the resistant tumor can be detected before reaching its initial size.

Most clinical trials report data on the distribution of recurrence time measured from the time of surgery (Avanzini and Antal, 2019) with drug therapy usually following after. Therefore, since only undetected secondary tumors are present at the time of treatment with anti-cancer drug, we lack data on the size of the tumors and cannot compare the empirical distributions to our predictions. However, we expect the variability of secondary tumors to average out across large cohorts of patients, thus we can use the mean recurrence time to compare with clinical data.

Discussion

We have modeled a tumor–a population of cancer cells–exposed to drug treatment that causes it to decline in size towards potential extinction. In this scenario, the tumor can be "evolutionary rescued", or escape extinction, via two paths. In the direct path, a sensitive cell acquires a mutation that confers resistance that allows it to rapidly grow. In the indirect path, a sensitive cell first becomes aneuploid, which diminishes the effect of the drug, and then an aneuploid cell acquires a mutation that confers resistance (Figure 1).

Evolutionary rescue Using multitype branching processes, we derived the probability of evolutionary rescue of the tumor under effects of aneuploidy, ranging from tolerance to partial resistance. We obtained exact and approximate expressions for the probability of evolutionary rescue (eq. (2)). Our results show that the probability of evolutionary rescue increases with the initial tumor size N, the sensitive growth rate Δ_w, the mutation rate v, and the aneuploidy rate u.

When aneuploid cells are partially resistant to the drug ($\Delta_w \ll 0 \ll \Delta_a \ll \Delta_m$), aneuploidy itself rescues the population (Figure 4A). When aneuploidy only provides tolerance to the drug ($\Delta_w \ll \Delta_a \ll 0 \ll \Delta_m$), it cannot rescue the population. Instead, it acts as a *stepping stone* through which the resistant mutant can appear more rapidly, given that the aneuploid cell population size declines slower then that of the sensitive cell population (Figure 2). In this scenario, aneuploidy provides two benefits. First, it delays the extinction of the population, providing more time for appearance of the resistance mutation. Second, it increases the population size relative to a sensitive population, providing more cells in which mutations can occur, i.e., it increases the mutation supply (i.e., $Nuv\lambda_w\lambda_a/|\Delta_w\Delta_a|$).

We find that aneuploidy can have a significant effect on evolutionary rescue as it reduces the threshold tumor size by at least an order-of-magnitude even when aneuploidy only provides tolerance (Figure 3). Interestingly, aneuploidy is unlikely to contribute to evolutionary rescue in primary tumors in which the number of cells is large enough (i.e., $N \gg N_m^* \approx 4 \times 10^7$) for the appearance of resistant mutation in sensitive cells before these cells become extinct (Figure 3). However, aneuploidy can have a crucial role in the evolutionary rescue of secondary tumors, in which the number of sensitive cells may be below the detection threshold of $\sim 10^7$ (Bozic et al., 2013), and this can have an impact on the recurrence of cancer after the resection of the primary tumor through secondary tumors, which are

too small to be detected and for which chemotherapy is employed to prevent cancer relapse. These secondary tumors are estimated to cause the majority of cancer-related deaths (Chaffer and Weinberg, 2011). The importance of aneuploidy in the evolutionary rescue of secondary tumors is reinforced by the fact that metastases have been shown to have a chromosome missegregation rate two to three orders of magnitude higher then that of primary tumors (Kimmel et al., 2023).

Given the fact that the mean time for secondary tumors to overcome chemotherapy can be of the order of 1,000 days (Figure S2A), aneuploidy can explain the reappearance of cancer even after initial remission. The theoretical prediction for the mean rescue time for tumors smaller then 10^8 cells is greater than 4 years, consistent with previous estimates of the recurrence time of tumors after resection (Avanzini and Antal, 2019). We found that aneuploidy complements evolutionary rescue through direct mutation because it generates rescue mutations mostly after the wildtype population had died out and direct mutation is no longer a viable option for evolutionary rescue (Figure 6A).

We hypothesized that *standing genetic variation* (the existence of a subpopulation of aneuploid cancer cells before the onset of therapy) can facilitate evolutionary rescue by reducing the waiting time for the appearance of aneuploid cells. We found that a drug or combination of drugs that reduces the wildtype growth rate and does not significantly increase the chromosome missegregation rate is more likely to cause evolutionary rescue to occur through direct mutation (eq. (6)). Furthermore, we found that for reasonable parameter values evolutionary rescue is more likely to occur through *de-novo* aneuploidy (Figure 5). If the fraction of tumor cells that have the beneficial aneuploidy is $f \gg \frac{u\lambda_w}{|\Delta_w|} \approx 2.5\%$, then evolutionary rescue is more likely to occur via standing variation, rather then through *de-novo* aneuploidy. In this scenario, evolutionary rescue likely occurs via aneuploid cells that acquire a resistance mutation and the probability of evolutionary rescue declines exponentially with initial tumor size (the probability of evolutionary rescue is given by $1 - \exp\left(-N/\tilde{N}_a^*\right)$, see Figure S5).

Experimental future direction Our model predictions could be tested by experiments (Martin et al., 2013). For example, to assess the effect of initial tumor size on the probability of evolutionary rescue, a large culture mass can be propagated from a single cancer cell in permissive conditions and then diluted to a range of starting tumor sizes. Then, these tumors may be exposed to anti-cancer drugs that induce aneuploidy or to saline solution for control (Ippolito et al., 2021). Cell density can be measured by optical density and a population exposed to the drug is considered extinct if the optical density is lower when compared to the control case with no cells present. We can then compare the results of the experiments to the predictions of our model to see if tumors with initial size bellow the threshold eq. (4) are more likely to become extinct due to the drug.

Additionally, our model predictions can be tested with data from patients. Given the type of cancer and how beneficial aneuploidy is, our model can predict the probability for cancer relapse after treatment.

Directions of future research Our model can be extended to understand evolutionary rescue in different biological contexts, for example, how yeast populations under stress overcome extinction via aneuploidy (Kohanovski et al., 2024, Pompei and Cosentino Lagomarsino, 2023). Additionally, we did not account for the heterogeneity of aneuploidy as not all aneuploid lineages have the same growth rate Δ_a as assumed in our model (Avecilla et al., 2023, Yang et al., 2021). Such heterogeneity can be accounted for by sampling the aneuploidy growth or death rates from a distribution (Martin et al., 2013).

We have assumed that cancer cell lineages are independent and have verified that this is accurate under simple logistic growth. However, this assumption neglects potential effects of spatial structure and local interactions, which may be important in solid tumors. Such tumors can be spatially heterogeneous with different genotypes inhabiting cellular niches and immune infiltration impacting growth in affected regions (Galon et al., 2010, Varrone et al., 2023). This has the potential to impact

the probability of evolutionary rescue (Martens et al., 2011).

An additional extension of our model could incorporate a wider range of parameters, however parameter values for different types of tumors are difficult to obtain.

Conclusions Our results quantitatively show that aneuploidy plays an important role in tumors overcoming exposure to chemotherapeutic drugs when tumor size is small or intermediate. Large tumors can escape anti-cancer drugs through direct mutation while smaller ones are able to obtain a resistance mutation through an aneuploid *stepping stone* (Figure 3). As a result, therapies that increase the rate of aneuploidy in tumors to combat cancer may have an adverse effect on patient outcomes.

Acknowledgements

We thank Hildegard Uecker for discussions and comments. This work was supported in part by the Israel Science Foundation (ISF 552/19, YR), the US–Israel Binational Science Foundation (BSF 2021276, YR), Minerva Stiftung Center for Lab Evolution (YR), Ela Kodesz Institute for Research on Cancer Development and Prevention (RS), the Simons Foundation (Investigator in Mathematical Modeling of Living Systems #508600, DBW), the Sloan Foundation (Research Fellowship FG-2021-16667, DBW), the National Science Foundation (grant #2146260, DBW),

References

Allen, L. J. (2010), *An introduction to stochastic processes with applications to biology*, CRC press.

Avanzini, S. and Antal, T. (2019), 'Cancer recurrence times from a branching process model', *PLoS computational biology* **15**(11), e1007423.

Avecilla, G., Spealman, P., Matthews, J., Caudal, E., Schacherer, J. and Gresham, D. (2023), 'Copy number variation alters local and global mutational tolerance', *Genome Research* **33**(8), 1340–1353.

Bakker, B., Schubert, M., Bolhaqueiro, A. C., Kops, G. J., Spierings, D. C. and Foijer, F. (2023), 'Predicting CIN rates from single-cell whole genome sequencing data using an *in silico* model', *bioRxiv* pp. 2023–02.

Barton, G. (1989), *Elements of Green's functions and propagation: potentials, diffusion, and waves*, Oxford University Press.

Ben-David, U. and Amon, A. (2020), 'Context is everything: aneuploidy in cancer', *Nature Reviews Genetics* **21**(1), 44–62.

Bozic, I., Reiter, J. G., Allen, B., Antal, T., Chatterjee, K., Shah, P., Moon, Y. S., Yaqubie, A., Kelly, N., Le, D. T. et al. (2013), 'Evolutionary dynamics of cancer in response to targeted combination therapy', *eLife* **2**, e00747.

Brauner, A., Fridman, O., Gefen, O. and Balaban, N. Q. (2016), 'Distinguishing between resistance, tolerance and persistence to antibiotic treatment', *Nature Reviews Microbiology* **14**(5), 320–330.

Carja, O. and Plotkin, J. B. (2017), 'The evolutionary advantage of heritable phenotypic heterogeneity', *Scientific reports* **7**(1), 1–12.

Carja, O. and Plotkin, J. B. (2019), 'Evolutionary rescue through partly heritable phenotypic variability', *Genetics* **211**(3), 977–988.

Carlson, J. A. (2003), 'Tumor doubling time of cutaneous melanoma and its metastasis', *The American journal of dermatopathology* **25**(4), 291–299.

Chaffer, C. L. and Weinberg, R. A. (2011), 'A perspective on cancer cell metastasis', *science* **331**(6024), 1559–1564.

Chevin, L.-M. (2011), 'On measuring selection in experimental evolution', *Biology letters* **7**(2), 210–213.

Cobbold, C. A. and Stana, R. (2020), 'Should I stay or should I go: partially sedentary populations can outperform fully dispersing populations in response to climate-induced range shifts', *Bulletin of Mathematical Biology* **82**(2), 1–21.

Del Monte, U. (2009), 'Does the cell number 10^9 still really fit one gram of tumor tissue?', *Cell cycle* **8**(3), 505–506.

Galon, J., Dieu-Nosjean, M., Tartour, E., Sautes-Fridman, C., Fridman, W. et al. (2010), 'Immune infiltration in human tumors: a prognostic factor that should not be ignored', *Oncogene* **29**(8), 1093–1102.

Giam, M. and Rancati, G. (2015), 'Aneuploidy and chromosomal instability in cancer: a jackpot to chaos', *Cell division* **10**(1), 1–12.

Gillespie, D. T. (1976), 'A general method for numerically simulating the stochastic time evolution of coupled chemical reactions', *Journal of computational physics* **22**(4), 403–434.

Gillespie, D. T. (1977), 'Exact stochastic simulation of coupled chemical reactions', *The journal of physical chemistry* **81**(25), 2340–2361.

Gillespie, D. T. (2001), 'Approximate accelerated stochastic simulation of chemically reacting systems', *The Journal of chemical physics* **115**(4), 1716–1733.

Gisselsson, D., Jin, Y., Lindgren, D., Persson, J., Gisselsson, L., Hanks, S., Sehic, D., Mengelbier, L. H., Øra, I., Rahman, N. et al. (2010), 'Generation of trisomies in cancer cells by multipolar mitosis and incomplete cytokinesis', *Proceedings of the National Academy of Sciences* **107**(47), 20489–20493.

Gomulkiewicz, R. and Holt, R. D. (1995), 'When does evolution by natural selection prevent extinction?', *Evolution* pp. 201–207.

Gunnarsson, E. B., De, S., Leder, K. and Foo, J. (2020), 'Understanding the role of phenotypic switching in cancer drug resistance', *Journal of theoretical biology* **490**, 110162.

Harris, T. E. (1963), *The theory of branching processes*, Vol. 6, Springer Berlin.

Harsch, M. A., Zhou, Y., HilleRisLambers, J. and Kot, M. (2014), 'Keeping pace with climate change: stage-structured moving-habitat models', *The American Naturalist* **184**(1), 25–37.

Ippolito, M. R., Martis, V., Martin, S., Tijhuis, A. E., Hong, C., Wardenaar, R., Dumont, M., Zerbib, J., Spierings, D. C., Fachinetti, D. et al. (2021), 'Gene copy-number changes and chromosomal instability induced by aneuploidy confer resistance to chemotherapy', *Developmental cell* **56**(17), 2440–2454.

Kimmel, G. J., Beck, R. J., Yu, X., Veith, T., Bakhoum, S., Altrock, P. M. and Andor, N. (2023), 'Intratumor heterogeneity, turnover rate and karyotype space shape susceptibility to missegregation-induced extinction', *PLOS Computational Biology* **19**(1), e1010815.

Kocarnik, J. M., Compton, K., Dean, F. E., Fu, W., Gaw, B. L., Harvey, J. D., Henrikson, H. J., Lu, D., Pennini, A., Xu, R. et al. (2022), 'Cancer incidence, mortality, years of life lost, years lived with disability, and disability-adjusted life years for 29 cancer groups from 2010 to 2019: a systematic analysis for the global burden of disease study 2019', *JAMA oncology* **8**(3), 420–444.

Kohanovski, I., Pontz, M., Vande Zande, P., Selmecki, A., Dahan, O., Pilpel, Y., Yona, A. H. and Ram, Y. (2024), 'Aneuploidy can be an evolutionary diversion on the path to adaptation', *Molecular Biology and Evolution* p. msae052.

Lee, H.-S., Lee, N. C., Kouprina, N., Kim, J.-H., Kagansky, A., Bates, S., Trepel, J. B., Pommier, Y., Sackett, D. and Larionov, V. (2016), 'Effects of anticancer drugs on chromosome instability and new clinical implications for tumor-suppressing therapies', *Cancer research* **76**(4), 902–911.

Levien, E., Min, J., Kondev, J. and Amir, A. (2021), 'Non-genetic variability in microbial populations: survival strategy or nuisance?', *Reports on Progress in Physics* **84**(11), 116601.

Loeb, L. A. (2001), 'A mutator phenotype in cancer', *Cancer research* **61**(8), 3230–3239.

Lukow, D. A., Sausville, E. L., Suri, P., Chunduri, N. K., Wieland, A., Leu, J., Smith, J. C., Girish, V., Kumar, A. A., Kendall, J. et al. (2021), 'Chromosomal instability accelerates the evolution of resistance to anti-cancer therapies', *Developmental cell* **56**(17), 2427–2439.

Martens, E. A., Kostadinov, R., Maley, C. C. and Hallatschek, O. (2011), 'Spatial structure increases the waiting time for cancer', *New journal of physics* **13**(11), 115014.

Martin, G., Aguilée, R., Ramsayer, J., Kaltz, O. and Ronce, O. (2013), 'The probability of evolutionary rescue: towards a quantitative comparison between theory and evolution experiments', *Philosophical Transactions of the Royal Society B: Biological Sciences* **368**(1610), 20120088.

Mason, J. M., Wei, X., Fletcher, G. C., Kiarash, R., Brokx, R., Hodgson, R., Beletskaya, I., Bray, M. R. and Mak, T. W. (2017), 'Functional characterization of cfi-402257, a potent and selective mps1/ttk kinase inhibitor, for the treatment of cancer', *Proceedings of the National Academy of Sciences* **114**(12), 3127–3132.

Orr, H. A. and Unckless, R. L. (2008), 'Population extinction and the genetics of adaptation', *The American Naturalist* **172**(2), 160–169.

Orr, H. A. and Unckless, R. L. (2014), 'The population genetics of evolutionary rescue', *PLoS genetics* **10**(8), e1004551.

Pompei, S. and Cosentino Lagomarsino, M. (2023), 'A fitness trade-off explains the early fate of yeast aneuploids with chromosome gains', *Proceedings of the National Academy of Sciences* **120**(15), e2211687120.

Replogle, J. M., Zhou, W., Amaro, A. E., McFarland, J. M., Villalobos-Ortiz, M., Ryan, J., Letai, A., Yilmaz, O., Sheltzer, J., Lippard, S. J. et al. (2020), 'Aneuploidy increases resistance to chemotherapeutics by antagonizing cell division', *Proceedings of the National Academy of Sciences* **117**(48), 30566–30576.

Rew, D. and Wilson, G. (2000), 'Cell production rates in human tissues and tumours and their significance. part ii: clinical data', *European Journal of Surgical Oncology (EJSO)* **26**(4), 405–417.

Rutledge, S. D., Douglas, T. A., Nicholson, J. M., Vila-Casadesús, M., Kantzler, C. L., Wangsa, D., Barroso-Vilares, M., Kale, S. D., Logarinho, E. and Cimini, D. (2016), 'Selective advantage of trisomic human cells cultured in non-standard conditions', *Scientific reports* **6**(1), 22828.

Schukken, K. M. and Foijer, F. (2018), 'CIN and aneuploidy: different concepts, different consequences', *Bioessays* **40**(1), 1700147.

Smith, J. C. and Sheltzer, J. M. (2018), 'Systematic identification of mutations and copy number alterations associated with cancer patient prognosis', *elife* **7**, e39217.

Tanaka, M. M. and Wahl, L. M. (2022), 'Surviving environmental change: when increasing population size can increase extinction risk', *Proceedings of the Royal Society B* **289**(1976), 20220439.

Uecker, H. and Hermisson, J. (2011), 'On the fixation process of a beneficial mutation in a variable environment', *Genetics* **188**(4), 915–930.

Uecker, H. and Hermisson, J. (2016), 'The role of recombination in evolutionary rescue', *Genetics* **202**(2), 721–732.

Uecker, H., Otto, S. P. and Hermisson, J. (2014), 'Evolutionary rescue in structured populations', *The American Naturalist* **183**(1), E17–E35.

Uecker, H., Setter, D. and Hermisson, J. (2015), 'Adaptive gene introgression after secondary contact', *Journal of mathematical biology* **70**, 1523–1580.

Van Rossum, G. and Others (2007), Python programming language, *in* 'USENIX Annu. Tech. Conf.'.

Varrone, M., Tavernari, D., Santamaria-Martínez, A., Walsh, L. A. and Ciriello, G. (2023), 'Cellcharter reveals spatial cell niches associated with tissue remodeling and cell plasticity', *Nature Genetics* pp. 1–11.

Wang, S., Zhang, M., Liang, D., Sun, W., Zhang, C., Jiang, M., Liu, J., Li, J., Li, C., Yang, X. et al. (2019), 'Molecular design and anticancer activities of small-molecule monopolar spindle 1 inhibitors: A medicinal chemistry perspective', *European Journal of Medicinal Chemistry* **175**, 247–268.

Weissman, D. B., Desai, M. M., Fisher, D. S. and Feldman, M. W. (2009), 'The rate at which asexual populations cross fitness valleys', *Theoretical population biology* **75**(4), 286–300.

Weissman, D. B., Feldman, M. W. and Fisher, D. S. (2010), 'The rate of fitness-valley crossing in sexual populations', *Genetics* **186**(4), 1389–1410.

Wilson, B. A., Pennings, P. S. and Petrov, D. A. (2017), 'Soft selective sweeps in evolutionary rescue', *Genetics* **205**(4), 1573–1586.

Yang, F., Todd, R. T., Selmecki, A., Jiang, Y.-y., Cao, Y.-b. and Berman, J. (2021), 'The fitness costs and benefits of trisomy of each candida albicans chromosome', *Genetics* **218**(2), iyab056.

Zhou, Y. (2022), 'Range shifts under constant-speed and accelerated climate warming', *Bulletin of Mathematical Biology* **84**(1), 1.

	Name	Value	Units	References
N	Initial tumor size	$10^7 - 10^9$	cells	Del Monte (2009)
λ_w	Wildtype division rate	0.1	1/days	Bozic et al. (2013), Rew and Wilson (2000)
μ_w	Wildtype death rate	$0.11 - 0.17$	1/days	Bozic et al. (2013)
λ_a	Aneuploid division rate*	$0.06 - 0.1$	1/days	-
μ_a	Aneuploid death rate*	0.09	1/days	-
λ_m	Mutant division rate	0.1	1/days	Bozic et al. (2013), Rew and Wilson (2000)
μ_m	Mutant death rate	0.09	1/days	Bozic et al. (2013), Carlson (2003)
u	Missegregation rate	$10^{-3} - 10^{-2}$	1/cell division	Bakker et al. (2023)
v	Mutation rate	$10^{-9} - 10^{-7}$	1/cell division	Bozic et al. (2013), Loeb (2001)
$\tilde{u}$	Missegregation rate in the drug free environment*	2×10^{-3}	1/cell division	-
s	Selection coefficient of aneuploidy in the drug free environment	0.07	1/days	Lukow et al. (2021)

Table 1: Model parameters. We have modified the parameters from Bozic et al. (2013) such that wildtype/mutant division rate is $\lambda_{w,m} = \log 2/T \approx 0.1$ instead of their value of 0.14 where T is the doubling time in the absence of cellular death obtained from Rew and Wilson (2000).

Appendices

Appendix A Survival probability of a single lineage

To analyze evolutionary rescue in our model, we use the framework of *multitype branching processes* (Harris, 1963, Weissman et al., 2009). This allows us to find explicit expressions for the *survival probability*: the probability that a lineage descended from a single cell does not become extinct.

Let p_w, p_a, and p_m be the survival probabilities of a population consisting initially of single wildtype cell, aneuploid cell, or mutant cell, respectively. The complements $1-p_w$, $1-p_a$, and $1-p_m$ are the extinction probabilities, which satisfy each its respective equation (Harris, 1963),

$$\begin{aligned}
1-p_w =& \frac{\mu_w}{\lambda_w+\mu_w+u\lambda_w+v\lambda_w} + \frac{u\lambda_w}{\lambda_w+\mu_w+u\lambda_w+v\lambda_w}\left(1-p_a\right)\left(1-p_w\right) + \\
& \frac{\lambda_w}{\lambda_w+\mu_w+u\lambda_w+v\lambda_w}\left(1-p_w\right)^2 + \frac{v\lambda_w}{\lambda_w+\mu_w+u\lambda_w+v\lambda_w}\left(1-p_m\right)\left(1-p_w\right), \\
1-p_a =& \frac{\mu_a}{\lambda_a+\mu_a+v\lambda_a} + \frac{v\lambda_a}{\lambda_a+\mu_a+v\lambda_a}\left(1-p_m\right)\left(1-p_a\right) + \frac{\lambda_a}{\lambda_a+\mu_a+v\lambda_a}\left(1-p_a\right)^2, \\
1-p_m =& \frac{\mu_m}{\lambda_m+\mu_m} + \frac{\lambda_m}{\lambda_m+\mu_m}\left(1-p_m\right)^2.
\end{aligned} \tag{A1}$$

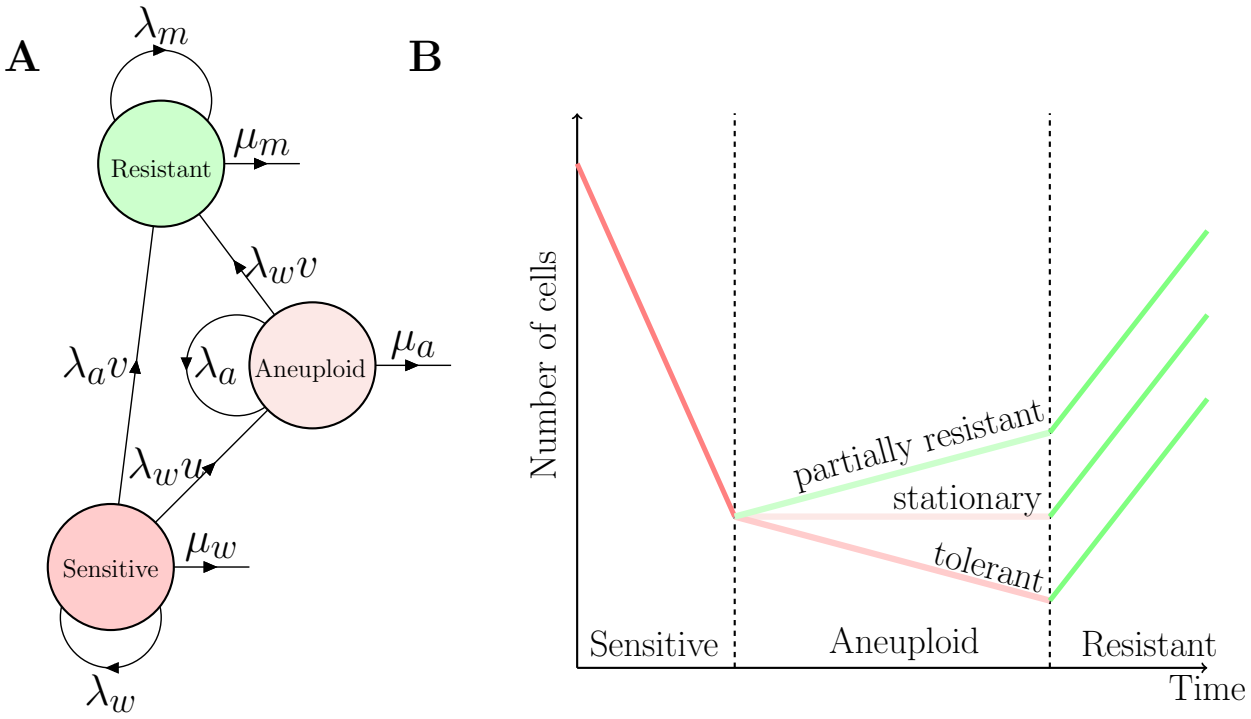

Figure 1: Model illustration. **(A)** A population of cancer cells is composed of wildtype, aneuploid, and mutant cells, which divide with rates λ_w, λ_a, and λ_m and die at rates μ_w, μ_a, and μ_m, respectively. Wildtype cells can divide and become aneuploid at rate $u\lambda_w$. Both aneuploid and wildtype cells can divide and acquire a mutation with rate $v\lambda_a$ and $v\lambda_w$, respectively. Color denotes the relative growth rates of the three genotypes such that $\lambda_w - \mu_w < \lambda_a - \mu_a < \lambda_m - \mu_m$. **(B)** The wildtype and the mutant are susceptible and resistant, respectively, to the drug. The aneuploid may be tolerant, stationary and partially resistant.

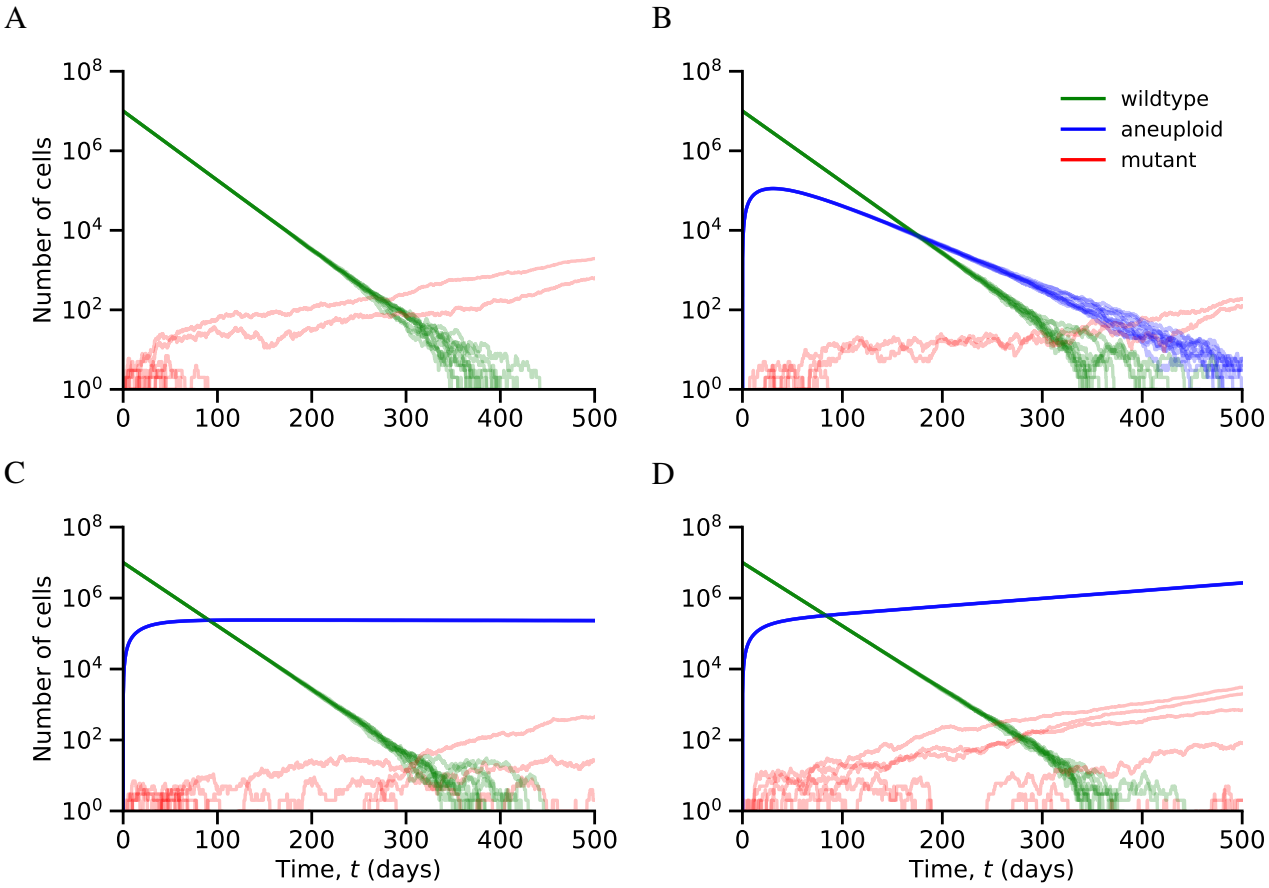

Figure 2: Sample trajectories of the different genotype frequencies. (A) Without aneuploidy ($u = 0$) evolutionary rescue is possible through direct mutation and in most scenarios the tumor will become extinct due to the drug. (B) When aneuploid cells are tolerant ($\Delta_a < 0$), we observe that, similar to A, direct mutation is the only path for evolutionary rescue. (C) When aneuploid cells are stationary ($\Delta_a \approx 0$), we observe the appearance of aneuploid lineages even after the wildtype population has gone extinct, thus showing that stationary aneuploidy increases the probability of evolutionary rescue. (D) When aneuploid cells are partially resistant ($\Delta_a > 0$), the tumor is rescued by the aneuploid cell population. Each plot shows 10 simulations of the number of wildtype, aneuploid and mutant cells (w_t, a_t, m_t) over time t with the following parameter values: $\lambda_w = 0.1, \lambda_m = 0.1, \mu_w = 0.14, \mu_a = 0.09, \mu_m = 0.09, v = 10^{-7}, N = 10^7$. For (A) we set $u = 0$, for (B) $\lambda_a = 0.065, u = 10^{-2}$, for (C) $\lambda_a = 0.0899, u = 10^{-2}$ and for (D) $\lambda_a = 0.095, u = 10^{-2}$.

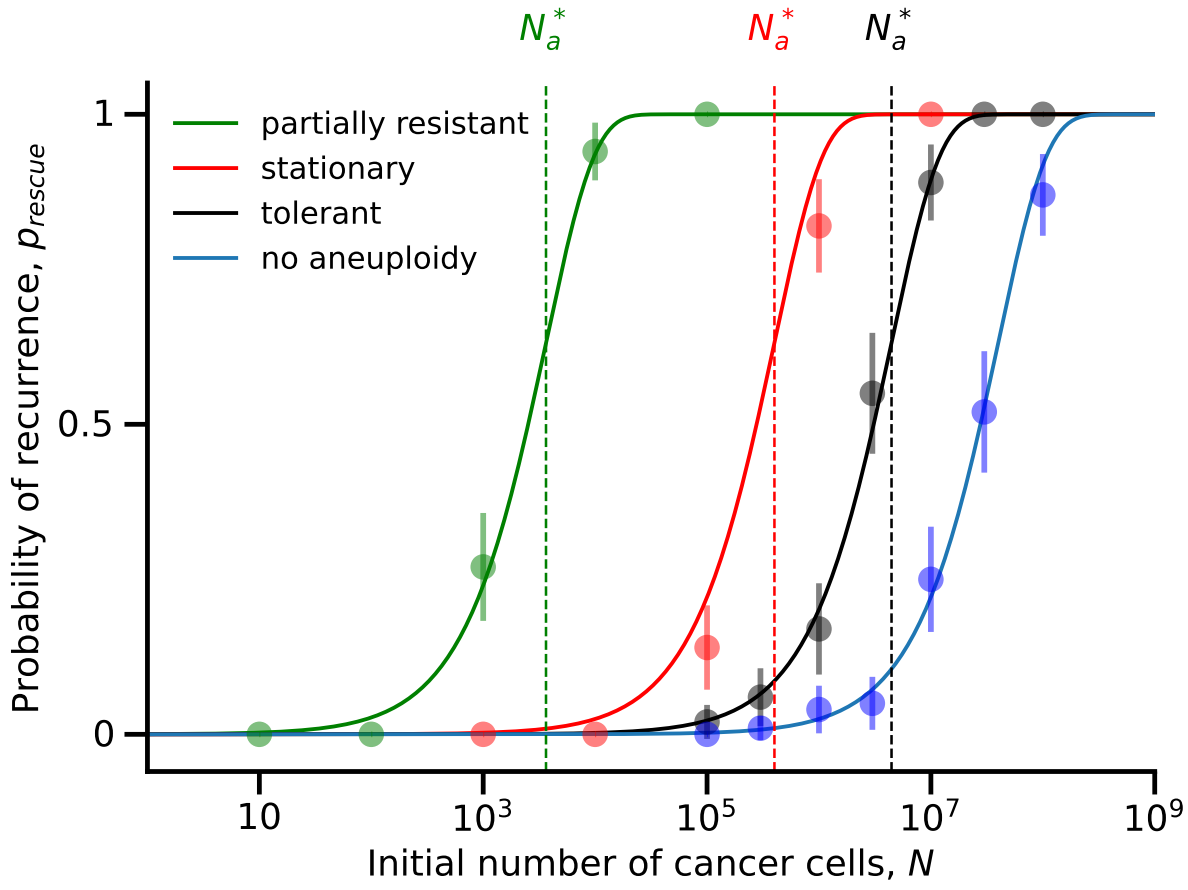

Figure 3: Aneuploidy facilitates evolutionary rescue of cancer under drug treatment. The probability of evolutionary rescue (i.e., the probability that the population does not become extinct), p_{rescue}, as a function of the initial tumor size, N (eq. (2)). Dashed vertical line shows the threshold tumor size, N_a^*, above which the probability is very high (eq. (4)). Blue dashed line: without aneuploidy ($u = 0$). Black line: tolerant aneuploidy ($u = 10^{-2}, \lambda_a = 0.0899$). Red line: stationary aneuploidy ($u = 10^{-2}, \lambda_a = 0.08999$). Green line represents the scenario with partially resistant aneuploidy ($u = 10^{-2}, \lambda_a = 0.095$). Dots for simulations and the error bars for 95% confidence interval ($p \pm 1.96\sqrt{p\left(1-p\right)/n}$ where p is the fraction of simulations in which the tumor has been rescued and $n = 100$ is the number of simulations). Parameters: $\lambda_w = 0.1, \lambda_m = 0.1, \mu_w = 0.14, \mu_a = 0.09, \mu_m = 0.09, \nu = 10^{-7}$.

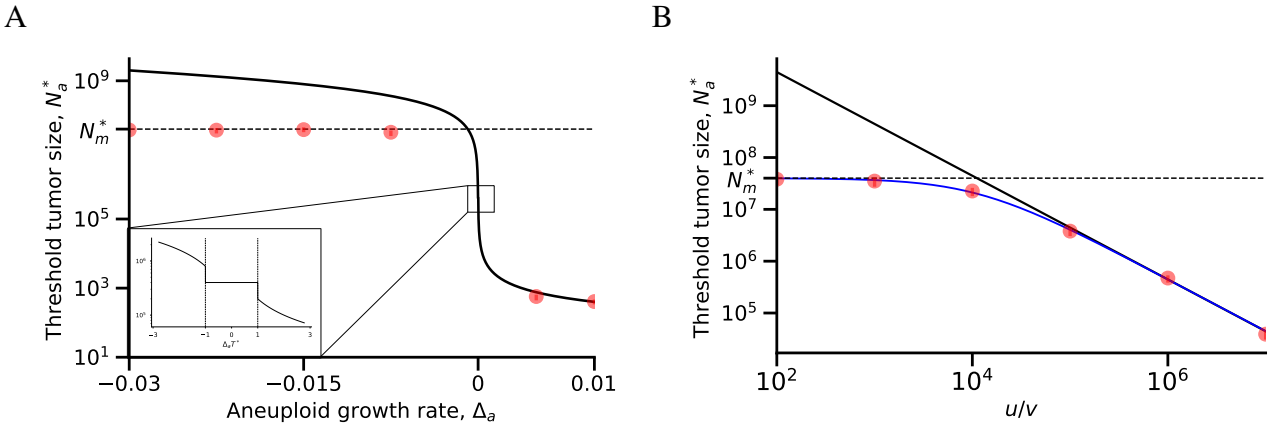

Figure 4: The effect of aneuploidy on tumor threshold size. (A) The threshold tumor size N_a^* as a function of the aneuploid growth rate Δ_a. The dashed horizontal line shows N_m^*, the threshold tumor size without aneuploidy ($u = 0$). When aneuploid growth rate is close to or higher than zero, aneuploidy decreases the threshold tumor size, thereby facilitating evolutionary rescue. The inset highlights the scenario when aneuploid cells are stationary. Red dots for simulations and error bars for the 95% confidence intervals obtained with bootstrap (Appendix G). Parameters: $\lambda_w = 0.1, \lambda_m = 0.1, \mu_w = 0.14, \mu_a = 0.09, \mu_m = 0.09, u = 10^{-2}, v = 10^{-7}$. (B) Threshold tumor size N_a^* as a function of the ratio of aneuploidy and mutation rates, u/v. Dashed horizontal line shows N_m^*, the threshold tumor size without aneuploidy ($u = 0$). When the aneuploidy rate is much higher than the mutation rate, aneuploidy decreases the threshold tumor size, thereby facilitating evolutionary rescue. Blue line represents the exact formula for threshold tumor size N_a^* while the solid black line represents the approximation (eq. (4)). Red dots represents simulation results and the error bars represent the 95% confidence intervals obtained with bootstrap (Appendix G). Parameters: $\lambda_w = 0.1, \lambda_m = 0.0899, \lambda_m = 0.1, \mu_w = 0.14, \mu_a = 0.09, \mu_m = 0.09, v = 10^{-7}$.

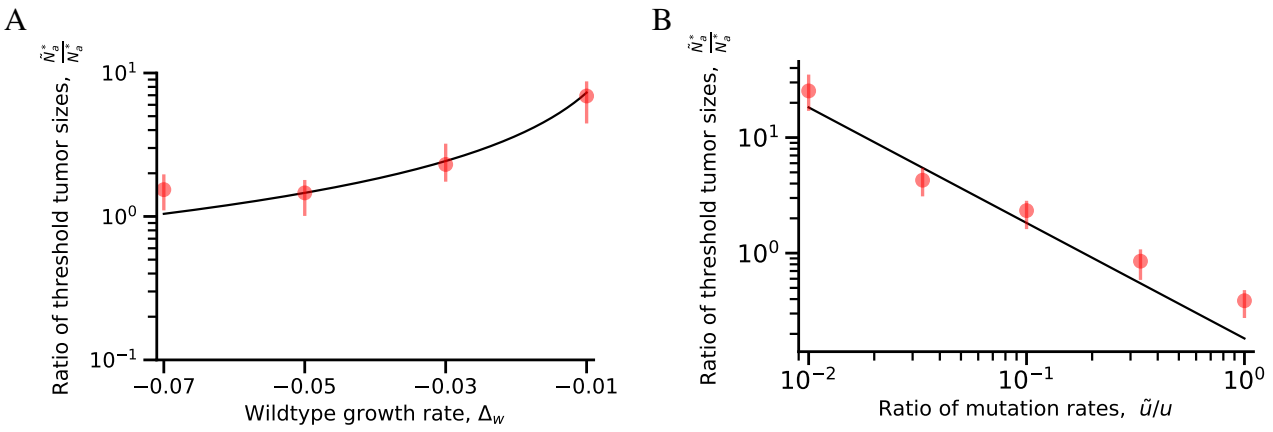

Figure 5: Standing genetic variation facilitates evolutionary rescue of cancer. (A) Ratio of threshold tumor size $\tilde{N}_a^*$ when a fraction $\frac{\tilde{u}\lambda_w}{s}$ is aneuploid at the start of treatment and N_a^* as a function of the wildtype growth rate Δ_w. Standing genetic variation will drive adaptation to the drug if the wildtype population is rapidly declining ($\Delta_w \ll 0$) due to a stronger effect of the drug on sensitive cells. Red dots represents simulation results and the error bars represent the 95% confidence intervals obtained with bootstrap (Appendix G). Parameters: $\lambda_w = 0.1, \lambda_a = 0.0899, \lambda_m = 0.1, \mu_a = 0.09, \mu_m = 0.09, \tilde{u} = 10^{-3}, u = 10^{-2}, v = 10^{-7}$. (B) Ratio of threshold tumor size $\tilde{N}_a^*$ when a fraction $\frac{\tilde{u}\lambda_w}{s}$ is aneuploid at the start of treatment and N_a^* as a function of the the ratio of aneuploidy rates $\tilde{u}/u$. *De-novo* aneuploids will have larger contribution to the appearance of drug resistance if the drug induces the appearance of aneuploid cells ($u \gg \tilde{u}$). Red dots represents simulation results and the error bars represent the 95% confidence intervals obtained with bootstrap (Appendix G). Parameters: $\lambda_w = 0.1, \lambda_a = 0.0899, \lambda_m = 0.1, \mu_w = 0.14, \mu_a = 0.09, \mu_m = 0.09, \tilde{u} = 10^{-3}, v = 10^{-7}$.

The survival probabilities are given by the smallest solution for each quadratic equation (Uecker et al., 2015). Therefore we have

$$
\begin{aligned}
p_w &= \frac{\lambda_w - \mu_w - u\lambda_w p_a - v\lambda_w p_m + \sqrt{\left(\lambda_w - \mu_w - u\lambda_w p_a - v\lambda_w p_m\right)^2 + 4\lambda_w^2\left(up_a + vp_m\right)}}{2\lambda_w}, \\
p_a &= \frac{\lambda_a - \mu_a - v\lambda_a p_m + \sqrt{\left(\lambda_a - \mu_a - v\lambda_a p_m\right)^2 + 4\lambda_a^2 v p_m}}{2\lambda_a}, \\
p_m &= \frac{\lambda_m - \mu_m}{\lambda_m}.
\end{aligned}
\tag{A2}
$$

Note that the equation for p_w depends on both p_a and p_m, and the equation for p_a depends on p_m. To proceed, we can plug the solution for p_m and p_a into the solution for p_w. We perform this for three different scenarios.

Scenario 1: Aneuploid cells are partially resistant

We first assume that aneuploidy provides partial resistance to drug therapy, $\lambda_a > \mu_a$, and that this resistance is significant, $\left(\lambda_a - \mu_a - v\lambda_a p_m\right)^2 > 4\lambda_a^2 v p_m$. We thus rewrite eq. (A2) as

$$
\begin{aligned}
p_w &= \frac{\lambda_w - \mu_w - u\lambda_w p_a - v\lambda_w p_m}{2\lambda_w}\left(1 - \sqrt{1 + \frac{4\lambda_w^2\left(vp_m + up_a\right)}{\left(\lambda_w - \mu_w - u\lambda_w p_a - v\lambda_w p_m\right)^2}}\right), \text{and} \\
p_a &= \frac{\lambda_a - \mu_a - v\lambda_a p_m}{2\lambda_a}\left(1 + \sqrt{1 + \frac{4\lambda_a^2 v p_m}{\left(\lambda_a - \mu_a - v\lambda_a p_m\right)^2}}\right).
\end{aligned}
$$

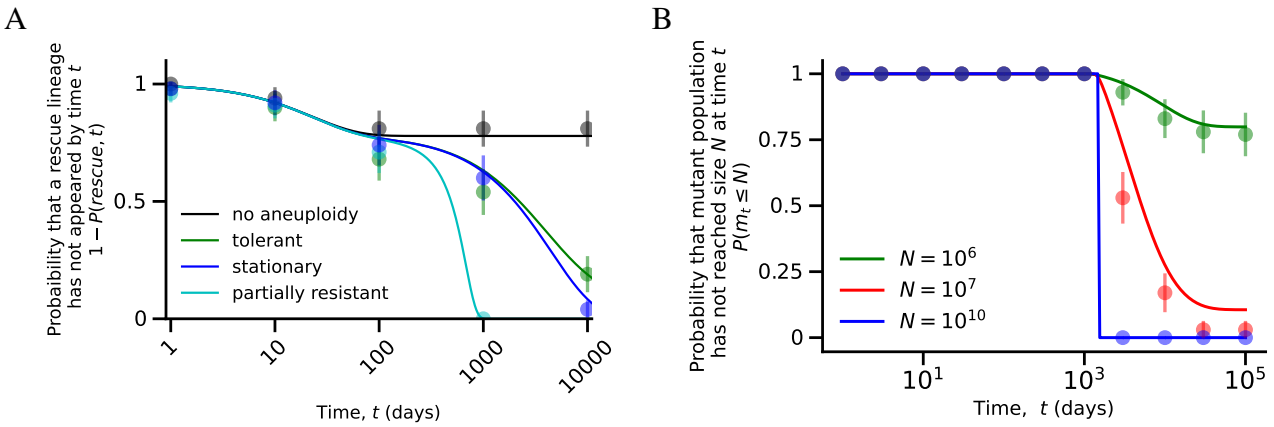

Figure 6: Aneuploidy extends the window of opportunity for evolutionary rescue. (A) The probability that a successful mutant has not appeared by time t. Green line: tolerant aneuploidy ($u > 0, \lambda_a = 0.0899$). Blue line: stationary aneuploidy ($u > 0, \lambda_a = 0.089999$). Cyan line: partially resistant aneuploidy ($u > 0, \lambda_a = 0.095$). Black line: no aneuploidy ($u = 0$). Aneuploidy starts to play an important role in rescuing the tumor cell population as the wildtype population becomes extinct. Markers represent simulation results and the error bars represent 95% confidence interval ($p \pm 1.96\sqrt{p\left(1-p\right)/n}$ where p is the fraction of simulations in which a successful mutant has not been generated and $n = 100$ is the number of simulations). Parameters: $\lambda_w = 0.1, \lambda_m = 0.1, \mu_w = 0.14, \mu_a = 0.09, \mu_m = 0.09, u = 10^{-2}, v = 10^{-7}, N = 10^7$. (B) Probability that a mutant cancer cell population has not reached size N at time t. Green line: $N = 10^6$ (small tumor). Red line: $N = 10^7$ (intermediate sized tumor). Blue line: $N = 10^{10}$ (large tumor). Increasing the initial tumor size guarantees that the cancer will relapse. Markers represent simulations and the error bars represents 95% confidence interval ($p \pm 1.96\sqrt{p\left(1-p\right)/n}$ where p is the fraction of the simulations in which the mutant population size has not reached N and $n = 100$ is the number of simulations). Parameters: $\lambda_w = 0.1, \lambda_a = 0.0899, \lambda_m = 0.1, \mu_w = 0.14, \mu_a = 0.09, \mu_m = 0.09, u = 10^{-2}, v = 10^{-7}$.

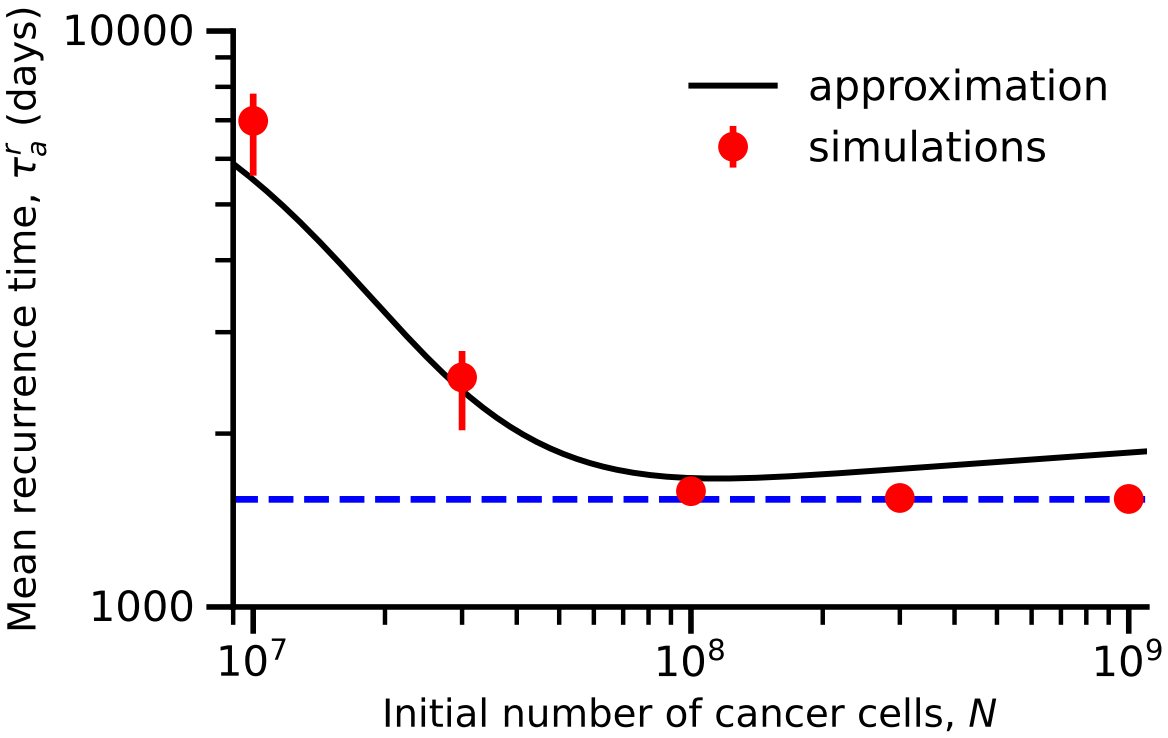

Figure 7: Tumor size decreases the mean recurrence time. The mean time for the mutant cell population to reach size N, the initial number of cancer cells. Our inhomogeneous Poisson-process approximation (solid black line, eq. (D1)) is in agreement with simulation results (red markers with 95% confidence interval obtained with bootstrapping, see Appendix G) for intermediary N. The simulations converge to eq. (D4) (blue dashed line) for large values of N. Parameters: $\lambda_w = 0.1, \lambda_a = 0.0899, \lambda_m = 0.1, \mu_w = 0.14, \mu_a = 0.09, \mu_m = 0.09, u = 10^{-2}, v = 10^{-7}$.

Using the Taylor expansion $\sqrt{1+x} = 1 + x/2 + O(x^2)$ and assuming $u, v \ll 1$, we obtain the following approximation for the survival probability of a population initially consisting of a single wildtype cell,

$$\begin{aligned} p_w &\approx -\frac{v\lambda_w p_m + u\lambda_w p_a}{\lambda_w - \mu_w - u\lambda_w p_a - v\lambda_w p_m} \\ &\approx -\frac{1}{\lambda_w - \mu_w}\left[\frac{u\lambda_w\left(\lambda_a - \mu_a\right)}{\lambda_a} + \frac{uv\lambda_w\lambda_a\left(\lambda_m - \mu_m\right)}{\lambda_m\left(\lambda_a - \mu_a\right)} + \frac{v\lambda_w\left(\lambda_m - \mu_m\right)}{\lambda_m}\right]. \end{aligned} \tag{A3}$$

Now uv is very small, and if we use the fact that $v \ll u$, we have:

$$p_w \approx \frac{u\lambda_w}{|\Delta_w|}\frac{\Delta_a}{\lambda_a}. \tag{A4}$$

However, if aneuploidy is very rare such that

$$\frac{u\lambda_w\Delta_a}{\lambda_a} < \frac{v\lambda_w\Delta_m}{\lambda_m} \Rightarrow u\lambda_a < \frac{v\lambda_a^2\Delta_m}{\lambda_m}\frac{1}{\Delta_a} < \frac{v\lambda_a^2\Delta_m}{\lambda_m}\frac{1}{\sqrt{4\lambda_a^2 v p_m}} \Rightarrow u\lambda_a < T^*,$$

where $T^* = (4v\lambda_a^2\Delta_m/\lambda_m)^{-1/2}$ and in the second inequality we used the fact that $\Delta_a^2 > 4\lambda_a^2 v p_m$. In this scenario adaptation is through direct mutation and:

$$p_w \approx \frac{v\lambda_w}{|\Delta_w|}\frac{\Delta_m}{\lambda_m}.$$

Scenario 2: Aneuploid cells are tolerant.

We now assume that aneuploidy provides tolerance to drug therapy, that is, the number of aneuploid cells significantly declines over time, but at a lower rate than the number of wildtype cells, $\lambda_w - \mu_w < \lambda_a - \mu_a < 0$. We also assume that the decline are significant, $\left(\lambda_a - \mu_a - v\lambda_a p_m\right)^2 > 4\lambda_a^2 v p_m$. We rewrite eq. (A2) as

$$\begin{aligned} p_w &= \frac{\lambda_w - \mu_w - u\lambda_w p_a - v\lambda_w p_m}{2\lambda_w}\left(1 - \sqrt{1 + \frac{4\lambda_w^2\left(v p_m + u p_a\right)}{\left(\lambda_w - \mu_w - u\lambda_w p_a - v\lambda_w p_m\right)^2}}\right), \\ p_a &= \frac{\lambda_a - \mu_a - v\lambda_a p_m}{2\lambda_a}\left(1 - \sqrt{1 + \frac{4\lambda_a^2 v p_m}{\left(\lambda_a - \mu_a - v\lambda_a p_m\right)^2}}\right). \end{aligned} \tag{A5}$$

Since $u, v \ll 1$, the term in the root can be approximated using a Taylor expansion. So, substituting the expressions for p_a and p_m, we have

$$\begin{aligned} p_w &\approx -\frac{v\lambda_w p_m + u\lambda_w p_a}{\lambda_w - \mu_w - u\lambda_w p_a - v\lambda_w p_m} \\ &\approx \frac{1}{\lambda_w - \mu_w - u\lambda_w p_a - v\lambda_w p_m}\left[\frac{uv\lambda_w\lambda_a\left(\lambda_m - \mu_m\right)}{\lambda_m\left(\lambda_a - \mu_a - v\lambda_a\right)} - \frac{v\lambda_w\left(\lambda_m - \mu_m\right)}{\lambda_m}\right] \\ &\approx \frac{v\lambda_w\left(\lambda_m - \mu_m\right)}{\lambda_m\left(\lambda_w - \mu_w\right)}\left[\frac{u\lambda_a}{\left(\lambda_a - \mu_a\right)} - 1\right] \\ &= \frac{v\lambda_w\Delta_m}{\lambda_m|\Delta_w|}\left(\frac{u\lambda_a}{|\Delta_a|} + 1\right). \end{aligned} \tag{A6}$$

If we assume that aneuploidy is not rare ($u\lambda_a > |\Delta_a|$) then we have:

$$p_w \approx \frac{u\lambda_w}{|\Delta_w|}\frac{v\lambda_a}{|\Delta_a|}\frac{\Delta_m}{\lambda_m}. \tag{A7}$$

Scenario 3: Aneuploid cells are stationary

We now assume that the growth rate of aneuploid cells is close to zero (either positive or negative), such that $\left(\Delta_a - v\lambda_a p_m\right)^2 \ll 4\lambda_a^2 v p_m$. We rewrite eq. (A2) as

$$p_a = \frac{\lambda_a - \mu_a - v\lambda_a p_m + 2\sqrt{\lambda_a^2 v p_m}\left(1 + \frac{\left(\lambda_a - \mu_a - v\lambda_a p_m\right)^2}{4\lambda_a^2 v p_m}\right)^{\frac{1}{2}}}{2\lambda_a}. \tag{A8}$$

Using a following Taylor series expansion for small $\left(\lambda_a - \mu_a - v\lambda_a p_m\right)^2 / 4\lambda_a^2 v p_m$,

$$\left(1 + \frac{\left(\lambda_a - \mu_a - v\lambda_a p_m\right)^2}{4\lambda_a^2 v p_m}\right)^{\frac{1}{2}} = 1 + \frac{\left(\lambda_a - \mu_a - v\lambda_a p_m\right)^2}{8\lambda_a^2 v p_m} + \cdots,$$

we obtain the approximation

$$\begin{aligned}
p_a &\approx \frac{\lambda_a - \mu_a - v\lambda_a p_m + 2\sqrt{\lambda_a^2 v p_m}\left[1 + \frac{\left(\lambda_a - \mu_a - v\lambda_a p_m\right)^2}{8\lambda_a^2 v p_m}\right]}{2\lambda_a} \\
&= \frac{\lambda_a - \mu_a - v\lambda_a p_m + 2\sqrt{\lambda_a^2 v p_m} + \frac{\left(\lambda_a - \mu_a - v\lambda_a p_m\right)^2}{4\sqrt{\lambda_a^2 v p_m}}}{2\lambda_a} \\
&= \frac{\left(\lambda_a - \mu_a - v\lambda_a p_m + 2\sqrt{\lambda_a^2 v p_m}\right)^2 + 4\lambda_a^2 v p_m}{8\lambda_a\sqrt{\lambda_a^2 v p_m}} \\
&= \frac{4\lambda_a^2 v p_m + 4\lambda_a^2 v p_m\left(1 + \frac{\lambda_a - \mu_a - v\lambda_a p_m}{2\sqrt{\lambda_a^2 v p_m}}\right)^2}{8\lambda_a\sqrt{\lambda_a^2 v p_m}} \\
&= \frac{1}{2\lambda_a}\left(\lambda_a - \mu_a - v\lambda_a p_m + 2\sqrt{\lambda_a^2 v p_m}\right).
\end{aligned} \tag{A9}$$

Plugging this in eq. (A3), the survival probability of a population starting from one wildtype cell is

$$\begin{aligned}
p_w &\approx -\frac{1}{\lambda_w - \mu_w - u\lambda_w p_a - v\lambda_w p_m}\left[v\lambda_w\frac{\lambda_m - \mu_m}{\lambda_m} + \frac{u\lambda_w}{2\lambda_a}\left(\lambda_a - \mu_a - v\lambda_a p_m + 2\sqrt{\lambda_a^2 v p_m}\right)\right] \\
&= -\frac{1}{\lambda_w - \mu_w - u\lambda_w - v\lambda_w}\left[v\lambda_w\frac{\lambda_m - \mu_m}{\lambda_m} + \frac{u\lambda_w}{2\lambda_a}\left(\lambda_a - \mu_a - v\lambda_a p_m\right) + u\lambda_w\sqrt{\frac{v\left(\lambda_m - \mu_m\right)}{\lambda_m}}\right] \\
&\approx -\frac{1}{\Delta_w}\left[v\lambda_w\frac{\Delta_m}{\lambda_m} + \frac{u\lambda_w\left(\Delta_a - v\lambda_a\right)}{2\lambda_a} + u\lambda_w\sqrt{\frac{v\Delta_m}{\lambda_m}}\right].
\end{aligned} \tag{A10}$$

Using the fact that

$$\left(\Delta_a - v\lambda_a p_m\right)^2 \ll 4\lambda_a^2 v p_m \Rightarrow \frac{\Delta_a - v\lambda_a p_m}{2\lambda_a} \ll \sqrt{\frac{v\lambda_a\Delta_m}{\lambda_m}},$$

and $v \ll u$ we obtain:

$$p_w \approx \frac{u\lambda_w}{|\Delta_w|}\sqrt{\frac{v\lambda_a\Delta_m}{\lambda_m}}. \tag{A11}$$

Appendix B Evolutionary rescue probability

Using the fact that $\Delta_a - v\lambda_a p_m \approx \Delta_a$ we write the condition $\left(\Delta_a - v\lambda_a p_m\right)^2 \ll 4\lambda_a^2 v p_m$ as:

$$\Delta_a^2 \ll 4\lambda_a^2 v p_m \Rightarrow -1 \ll \Delta_a T^* \ll 1,$$

where $T^* = (4v\lambda_a^2\Delta_m/\lambda_m)^{-1/2}$. Substituting eqs. (A4), (A7) and (A11) into eq. (2), the evolutionary rescue probability can be approximated by

$$p_{\text{rescue}} \approx \begin{cases} 1 - \exp\left[-\frac{u\lambda_a}{|\Delta_w|}\frac{v\lambda_w}{|\Delta_a|}\frac{\Delta_m}{\lambda_m}N\right], & \Delta_a T^* \ll -1, \\ 1 - \exp\left[-\frac{u\lambda_w}{|\Delta_w|}\sqrt{\frac{v\lambda_a\Delta_m}{\lambda_m}}N\right], & -1 \ll \Delta_a T^* \ll 1, \\ 1 - \exp\left[-\frac{u\lambda_w}{|\Delta_w|}\frac{\Delta_a}{\lambda_a}N\right], & 1 \ll \Delta_a T^*. \end{cases} \tag{B1}$$

Appendix C Evolutionary rescue time

We first calculate the expected time for the appearance of the first mutant that rescues the cell population. This can occur either through the evolutionary trajectory $wildtype \rightarrow mutant$ or through the trajectory $wildtype \rightarrow aneuploid \rightarrow mutant$. We start with the former.

Assuming no aneuploidy ($u = 0$), we define T_m to be the time at which the first mutant cell appears that will avoid extinction and will therefore rescue the population. Note that if extinction occurs, that is the frequency of mutants after a very long time is zero, $m_\infty = 0$, then it is implied that $T_m = \infty$, and vice versa if $T_m < \infty$ then $m_\infty > 0$.

The number of successful mutants generated until time t can be approximated by an inhomogeneous Poisson process with rate $R_m(t) = v\lambda_w p_m w_t$, where $w_t = N\mathrm{e}^{\Delta_w t}$ is the number of wildtype cells at time t. Note that

$$\int_0^t R_m(z)\mathrm{d}z = v\lambda_w p_m N\frac{\exp[\Delta_w t] - 1}{\Delta_w} \approx v\lambda_w p_m N t, \tag{C1}$$

by integrating the exponential and because $\frac{\exp[\Delta_w t]-1}{\Delta_w} = \frac{1+\Delta_w t+O(t^2)-1}{\Delta_w} = t + O(t^2)$. The probability density function of T_m is thus $R_m(t)\exp\left(-\int_0^t R_m(z)\mathrm{d}z\right)$ (Allen, 2010). Therefore, the probability density function of the conditional random variable $(T_m \mid T_m < \infty)$ is $f_m(t) = \frac{R_m(t)\exp\left(-\int_0^t R_m(z)\mathrm{d}z\right)}{p_{\text{rescue}}}$.

We are interested in the mean conditional time, $\tau_m = \mathbb{E}\left[T_m \mid T_m < \infty\right]$, which is given by

$$\tau_m = \int_0^\infty t f_m(t)\mathrm{d}t = \frac{\int_0^\infty t R_m(t)\exp\left(-\int_0^t R_m(z)\mathrm{d}z\right)\mathrm{d}t}{p_{rescue}}, \tag{C2}$$

Therefore, plugging eqs. (2) and (C1) in eq. (C2),

$$\tau_m = \int_0^\infty t v\lambda_w N\mathrm{e}^{\Delta_w t}\frac{\mathrm{e}^{-v\lambda_w N p_m\frac{\mathrm{e}^{\Delta_w t}-1}{\Delta_w}}}{1-\left(1-p_w\right)^N}\mathrm{d}t \approx \int_0^\infty t v\lambda_w N\mathrm{e}^{\Delta_w t}\frac{\mathrm{e}^{-v\lambda_w N p_m t}}{1-\mathrm{e}^{-N p_w}}\mathrm{d}t. \tag{C3}$$

Figure S2B show the agreement between this approximating and simulation results.
Assuming aneuploidy is possible ($u > 0$), we define T_a to be the time at which the first mutant cell appears that will rescue the population. We are interested in the mean conditional time, $\tau_a = \mathbb{E}\left[T_a \mid T_a < \infty\right]$.

When $Nu\lambda_w/|\Delta_w| \gg 1$ the aneuploid frequency dynamics is roughly deterministic and therefore can be approximated by

$$a_t \approx \frac{Nu\lambda_w}{\Delta_w - \Delta_a}\left(\mathrm{e}^{\Delta_w t} - \mathrm{e}^{\Delta_a t}\right). \tag{C4}$$

As a result, the number of successful mutants created by direct mutation and via aneuploidy can be approximated by inhomogeneous Poisson processes with the rates

$$r_1(t) = v\lambda_a p_m \int_0^t a_z \mathrm{d}z = \frac{uv\lambda_w\lambda_a N p_m}{\Delta_w - \Delta_a}\left(\frac{\mathrm{e}^{\Delta_w t} - 1}{\Delta_w} - \frac{\mathrm{e}^{\Delta_a t} - 1}{\Delta_a}\right), \tag{C5}$$

$$r_2(t) = v\lambda_w p_m \int_0^t w_z \mathrm{d}z = v\lambda_w N p_m \frac{\mathrm{e}^{\Delta_w t} - 1}{\Delta_w}. \tag{C6}$$

For large initial population sizes we assume that the two processes are independent and as a result, they can be merged into a single Poisson process with rate $R_a(t) = (r_1 + r_2)(t)$. Consequently, the mean time to the appearance of the first rescue mutant is

$$\begin{aligned}\tau_a &= \frac{\int_0^\infty t R_a(t) \exp\left(-\int_0^t R_a(z)\mathrm{d}z\right)\mathrm{d}t}{p_{rescue}} \\ &= \int_0^\infty t\left(v\lambda_a p_m a_t + v\lambda_w p_m w_t\right)\frac{\exp\left[-\frac{uv\lambda_w\lambda_a N p_m}{\Delta_w - \Delta_a}\left(\frac{\mathrm{e}^{\Delta_w t}-1}{\Delta_w} - \frac{\mathrm{e}^{\Delta_a t}-1}{\Delta_a}\right) - v\lambda_w N p_m \frac{\mathrm{e}^{\Delta_w t}-1}{\Delta_w}\right]}{1 - \mathrm{e}^{-Np_w}}\mathrm{d}t,\end{aligned} \tag{C7}$$

which we plot in Figure S2A as a function of the initial population size, N.

Paradoxically, we observe from Figure S2 that the mean time of a rescue mutation to appear is significantly shorter for the scenario when $u = 0$ when compared to the scenario $u > 0$, however this can be explained by the fact this mean time is conditioned on evolutionary rescue and, as a result, aneuploidy increase the *window of opportunity* in which a rescue mutation could appear thus increasing the mean time as well (Figure 2).

If $N \gg N_m^*$ then the mean time τ_a can be written as:

$$\tau_a = \int_0^\infty \mathrm{e}^{-R_a(\tau)}\,\mathrm{d}\tau = \int_0^\infty \exp\left[-\frac{uv\lambda_w\lambda_a N p_m}{\Delta_w - \Delta_a}\left(\frac{\mathrm{e}^{\Delta_w\tau} - 1}{\Delta_w} - \frac{\mathrm{e}^{\Delta_a\tau} - 1}{\Delta_a}\right) - v\lambda_w N p_m \frac{\mathrm{e}^{\Delta_w\tau} - 1}{\Delta_w}\right]\mathrm{d}\tau,$$

and we use the following Taylor series expansions:

$$\begin{aligned}\frac{\mathrm{e}^{\Delta_w\tau} - 1}{\Delta_w} &= \frac{1 + \Delta_w\tau + O(\tau^2) - 1}{\Delta_w} = \tau + O(\tau^2). \\ \frac{\mathrm{e}^{\Delta_a\tau} - 1}{\Delta_a} &= \frac{1 + \Delta_a\tau + O(\tau^2) - 1}{\Delta_a} = \tau + O(\tau^2),\end{aligned}$$

to obtain a simpler approximation for τ_a:

$$\tau_a \approx \int_0^\infty \mathrm{e}^{-v\lambda_w N p_m \tau}\,\mathrm{d}\tau = \frac{1}{v\lambda_w N p_m}. \tag{C8}$$

If $N \ll N_a^*$ then we can write Equation (C7) as:

$$\begin{aligned}\tau_a &\approx \frac{\int_0^\infty t v\lambda_a p_m a_\tau\,\mathrm{d}\tau}{1 - \mathrm{e}^{-Np_w}} \approx \frac{uv\lambda_a\lambda_w p_m|\Delta_w + \Delta_a|}{p_w\Delta_a^2\Delta_w^2} \\ &= \frac{1}{|\Delta_w|} + \frac{1}{|\Delta_a|},\end{aligned} \tag{C9}$$

where in the last line we used the fact that $1/p_w = N_a^*$ and Equation (4).

If a fraction f of the cancer cells are aneuploid when the drug is administered then the rates at which the rescue mutations are generated can be written as:

$$r_1^f(t) = v\lambda_a p_m \int_0^t a_z \mathrm{d}z = \left(1-f\right) \frac{uv\lambda_w\lambda_a N p_m}{\Delta_w - \Delta_a}\left(\frac{\mathrm{e}^{\Delta_w t}-1}{\Delta_w} - \frac{\mathrm{e}^{\Delta_a t}-1}{\Delta_a}\right) + fv\lambda_a N p_m \frac{\mathrm{e}^{\Delta_a t}-1}{\Delta_a},$$
$$r_2^f(t) = v\lambda_w p_m \int_0^t w_z \mathrm{d}z = \left(1-f\right) v\lambda_w N p_m \frac{\mathrm{e}^{\Delta_w t}-1}{\Delta_w},$$

and the mean evolutionary rescue time is given by:

$$\tilde{\tau}_a = \frac{\int_0^\infty t R_a^f(t) \exp\left(-\int_0^t R_a^f(z)\mathrm{d}z\right)\mathrm{d}t}{p_{rescue}}, \tag{C10}$$

where $R_a^f(t) = r_1^f(t) + r_2^f(t)$ and $p_{rescue} = 1 - \exp\left[-\left(1-f\right)p_w N - f p_a N\right]$. We plot our approximation in Figure S9 together with simulated data.

Appendix D Recurrence time

We define the proliferation time τ_a^p to be the time it takes the population of mutant cancer cells to reach the initial tumor size N. The number of rescue lineages generated by the wildtype population is given by eq. (C5) (see Figure S3):

$$r_1(\infty) = \frac{uv\lambda_w\lambda_a N p_m}{|\Delta_w||\Delta_a|} = \frac{N}{N_a^*},$$

where we ignore lineages created by direct mutation because we assumed $u\lambda_a > \max(-\Delta_a, 1/T^*)$, $N \ll N_m^*$ and used Equation (4).

This helps us distinguish between two scenarios for the proliferation time. Firstly, when we have at most one lineages which rescues the cancer cell population:

$$N \ll N_a^*.$$

As a result, the recurrence time is given by (Avanzini and Antal, 2019):

$$\tau_a^r \approx \tau_a + \frac{\log p_m N}{\Delta_m}. \tag{D1}$$

The factor of p_m in the second term of eq. (D1) is due to the fact that the lineage is conditioned to survive genetic drift and the time to reach N is shorter then the scenario without this property.

The second scenario is when the wildtype population produces a large number of rescue lineages in a short period of time. This is given by the condition:

$$N \gg N_a^*.$$

As a result, the recurrence time is obtained by solving the following system of ODEs:

$$\begin{aligned}
\frac{dw}{dt} &= \Delta_w w, \\
\frac{da}{dt} &= \Delta_a a + u\lambda_w w, \\
\frac{dm}{dt} &= \Delta_m m + v\lambda_a a + v\lambda_w w.
\end{aligned} \tag{D2}$$

Solving the system of ODEs for initial condition $\left(w(0), a(0), m(0)\right) = (N, 0, 0)$ we obtain:

$$m\left(t\right) = \frac{Nuv\lambda_a\lambda_w}{\Delta_w - \Delta_a}\left[\frac{\mathrm{e}^{\Delta_w t} - \mathrm{e}^{\Delta_m t}}{\Delta_w - \Delta_m} - \frac{\mathrm{e}^{\Delta_a t} - \mathrm{e}^{\Delta_m t}}{\Delta_a - \Delta_m}\right] + Nv\lambda_w\frac{\mathrm{e}^{\Delta_w t} - \mathrm{e}^{\Delta_m t}}{\Delta_w - \Delta_m}.$$

We obtain τ_a^r such that $m\left(\tau_a^r\right) = N$ by solving:

$$1 = \frac{uv\lambda_a\lambda_w}{\Delta_w - \Delta_a}\left[\frac{\mathrm{e}^{\Delta_w \tau_a^r} - \mathrm{e}^{\Delta_m \tau_a^r}}{\Delta_w - \Delta_m} - \frac{\mathrm{e}^{\Delta_a \tau_a^r} - \mathrm{e}^{\Delta_m \tau_a^r}}{\Delta_a - \Delta_m}\right] + v\lambda_w\frac{\mathrm{e}^{\Delta_w \tau_a^r} - \mathrm{e}^{\Delta_m \tau_a^r}}{\Delta_w - \Delta_m}. \tag{D3}$$

This is a transcendental equation which cannot be solved exactly but we can obtain an approximation by noting that for large τ_a^r the above equation can be written as:

$$1 = v\lambda_w\frac{\mathrm{e}^{\Delta_m \tau_a^r}}{|\Delta_w - \Delta_m|},$$

which has solution:

$$\tau_a^r \approx \frac{1}{\Delta_m}\log\frac{\Delta_m - \Delta_w}{v\lambda_w}. \tag{D4}$$

We observe that the terms given by the evolutionary trajectory $wildtype \rightarrow aneuploid \rightarrow mutant$ do not contribute to the above approximation and, as a result, we deduce that it accurate only for $N \gg N_m^* > N_a^*$.

Additionally, we note that if we are interested in the time until the tumor reaches a detectable size M then our above analysis is valid but in Equation (D1) we change:

$$\tau_a^{r,M} \approx \tau_a + \frac{\log p_m M}{\Delta_m}, \tag{D5}$$

and Equation (D4) becomes:

$$\tau_a^{r,M} \approx \frac{1}{\Delta_m}\log\frac{M\left(\Delta_m - \Delta_w\right)}{v\lambda_w N}, \tag{D6}$$

which we plot in Figure S8 and observe that our approximations are in agreement with simulations.

Appendix E Distribution of evolutionary rescue time

The probability that a successful mutant has been generated by time t is given by:

$$\begin{aligned} P\left(rescue, t\right) &= P\left(T_a < t\right) \\ &= 1 - \exp\left\{-\left[r_1\left(t\right) + r_2\left(t\right)\right]\right\} \\ &= 1 - \exp\left\{-\left[\frac{uv\lambda_w\lambda_a N p_m}{\Delta_w - \Delta_a}\left(\frac{\mathrm{e}^{\Delta_w t} - 1}{\Delta_w} - \frac{\mathrm{e}^{\Delta_a t} - 1}{\Delta_a}\right) + v\lambda_w N p_m\frac{\mathrm{e}^{\Delta_w t} - 1}{\Delta_w}\right]\right\}, \end{aligned}$$

where T_a is the time at which the first mutant cell appears that will avoid extinction and which was defined in appendix C.

As a result, the probability that a successful mutant has not been generated by time t is:

$$1 - P\left(rescue, t\right) = \exp\left\{-\left[\frac{uv\lambda_w\lambda_a N p_m}{\Delta_w - \Delta_a}\left(\frac{\mathrm{e}^{\Delta_w t} - 1}{\Delta_w} - \frac{\mathrm{e}^{\Delta_a t} - 1}{\Delta_a}\right) + v\lambda_w N p_m\frac{\mathrm{e}^{\Delta_w t} - 1}{\Delta_w}\right]\right\}. \tag{E1}$$

Appendix F Distribution of recurrence time

The probability distribution of the time that a lineage, consisting initially of a single cell, will reach size N as time t is given by the Gumbel distribution $\text{Gumb}_{max}\left(\frac{\log Np_m}{\Delta_m}, \frac{1}{\Delta_m}\right)$ (Avanzini and Antal, 2019) with probability density function:

$$G(t) = \mathrm{e}^{-p_m N \mathrm{e}^{-\Delta_m t}}.$$

A mutant lineage initiated at time s, through aneuploidy, at rate $v\lambda_a p_m a_s$ reaches size N before time t with probability $G(t-s)$ where $s \leq t$. As a result, the number of successful mutant lineages which reach size N by time t can be approximated by inhomogeneous Poisson random variable with rate:

$$r(t) = v\lambda_a p_m \int_0^t a_s G(t-s)\, \mathrm{d}s$$

where a_s is aneuploid population size at time s defined in eq. (C4). The proliferation time is defined as the first time the size of all lineages reaches N. When $N \ll |\Delta_w||\Delta_a| / uv\lambda_w\lambda_a p_m$ there is at most a single mutant lineage that will survive and reach size N (Figure S3) and the probability that the size of that lineage has not reached N by time t is given by:

$$\begin{aligned} P(m_t \leq N) &= \exp\left[-r(t)\right] \\ &= \exp\left[-\frac{Nuv\lambda_w\lambda_a p_m}{\Delta_w - \Delta_a} \int_0^t \left[\mathrm{e}^{\Delta_w s} - \mathrm{e}^{\Delta_a s}\right] \mathrm{e}^{-p_m N \mathrm{e}^{-\Delta_m (t-s)}}\, \mathrm{d}s\right]. \end{aligned} \tag{F1}$$

When $N \gg |\Delta_w||\Delta_a| / uv\lambda_w\lambda_a p_m$ the dynamics of the cancer cell populations is deterministic and approximated by the system of ODEs shown in eq. (D2). As a result, the size of the mutant cell population will always be below N until time τ_a^r and will always be greater after:

$$P(m_t \leq N) = 1 - H\left(t - \tau_a^r\right), \tag{F2}$$

where $H(x)$ is the Heaviside function:

$$H(x) = \begin{cases} 0, & x < 0, \\ 1, & x \geq 0. \end{cases}$$

We plot eq. (F1) and eq. (F2) in Figure Figure 6B and compare with stochastic simulations and observe that our approximation are in agreement.

We observe that for $N = 10^7$ our formula overestimates the probability that the mutant population will be smaller then N at time t. This can be explained by the fact that $N = 10^7$ is an intermediary scenario where the wildtype population produces a number of rescue lineages that is greater then one but still sufficiently small such that stochasticity plays an important role in the population dynamics. As a result, the number of mutant cancer cells will reach N faster then the scenario with a single mutant lineage. Additionally, we observe from Figure 6B that the probability of the mutant cell population reaching size N is approximately zero before time τ_a^r which is the recurrence time for the deterministic scenario. This can be explained as follows: in the deterministic scenario there is a sufficient number of lineages produced such that there exists a lineage where each descendant will only reproduce and not die; the time it takes for this lineage to reach N is the lower bound for the time of all other lineages to reach N and this time cannot be smaller then τ_a^r by definition. Given that for small values of N we expect that at most a single lineage will rescue the tumor, this lineage cannot reach N before τ_a^r for the deterministic scenario eq. (D4).

From eq. (F2) we obtain the distribution of the recurrence time conditional of evolutionary rescue:

$$f(t) = \frac{d}{dt}\left[\frac{P(m_t \geq N)}{p_{rescue}}\right] = r'(t)\, \frac{\exp\left[-r(t)\right]}{p_{rescue}}, \tag{F3}$$

which we plot in Figure S4 and compare with simulations. We note that in the scenario $N \gg |\Delta_w||\Delta_a| / uv\lambda_w\lambda_a p_m$ the distribution becomes the Dirac δ-function (Barton, 1989).

Appendix G: Bootstrapping

For the mean times the 95% confidence interval is obtained through bootstrapping in the following steps: (1) we simulate T 100 times; (2) we sample with replacement which we store in T'; (3) for each element of this sample we obtain $\tau = \mathbb{E}[T']$; (4) we repeat steps (2)-(3) 100 times to obtain τ and we select the upper and lower limits such that 95% of the values of τ lie in the interval given by the bounds.

For the threshold tumor sizes the 95% confidence interval is obtained through bootstrapping in the following steps: (1) we simulate p_{rescue} 100 times; (2) we sample with replacement which we store in S; (3) for each element of this sample we obtain $N_a^* = 1/p_w$ using $p_w = -1/N_s \log\left(1 - \bar{S}\right)$ where $\bar{S}$ is the mean of S and N_s is an arbitrary value of the initial population size we selected in order to calculate p_{rescue}; (4) we repeat steps (2)-(3) 100 times to obtain N_a^* and we select the upper and lower limits such that 95% of the values of N_a^* lie in the interval given by the bounds.

For the ratio of the threshold tumor sizes the 95% confidence interval is obtained through bootstrapping in the following steps: (1) we simulate p_{rescue} 100 times for both the scenario when $f = \tilde{u}\lambda_w/s$ and $f = 0$; (2) we sample with replacement which we store in S_f and S_0; (4) for each element of S_0 we obtain $N_a^* = 1/p_w$ using $p_w = -1/N_s \log\left(1 - \bar{S}\right)$ where $\bar{S}$ is the mean of S_0 and N_s is an arbitrary value of the initial population size we selected in order to calculate p_{rescue}; (5) for each element of S_f we obtain $\tilde{N}_a^* = 1/p_a$ using $p_a = -f/N_s \log\left(1 - \bar{S}\right)$ where $\bar{S}_f$ is the mean of S_f and N_s is an arbitrary value of the initial population size we selected in order to calculate p_{rescue}; (6) we repeat steps (2)-(5) 100 times to obtain $\tilde{N}_a^*/N_a^*$ and we select the upper and lower limits such that 95% of the values of $\tilde{N}_a^*/N_a^*$ lie in the interval given by the bounds.

Supplementary Figures

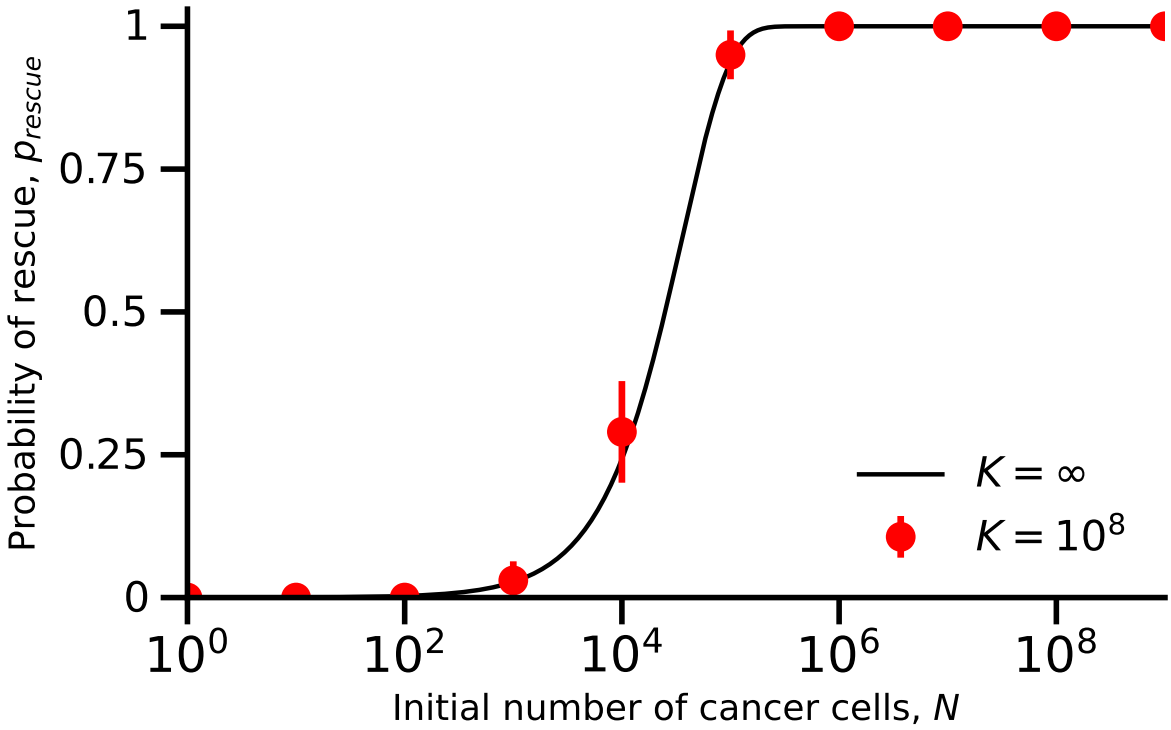

Figure S1: Density dependent growth does not affect the accuracy of our model. Comparison of results of simulations with density-dependent growth (red markers with with 95% CI) and the approximation formula (black line, eq. (4) in eq. (2)) with maximum carrying capacity $K = 10^8$ and effective carrying capacity $K_e = K\Delta_a/\lambda_a \approx 10^6$. The error bars represent 95% confidence interval of the form $p \pm 1.96\sqrt{p\left(1-p\right)/n}$ where p is the fraction of simulations in which the tumor has adapted to the stress and $n = 100$ is the number of simulations. Parameters: $\lambda_w = 0.1, \lambda_a = 0.0901, \lambda_m = 0.1, \mu_w = 0.14, \mu_a = 0.09, \mu_m = 0.09, u = 10^{-2}, v = 10^{-7}, K = 10^8$.

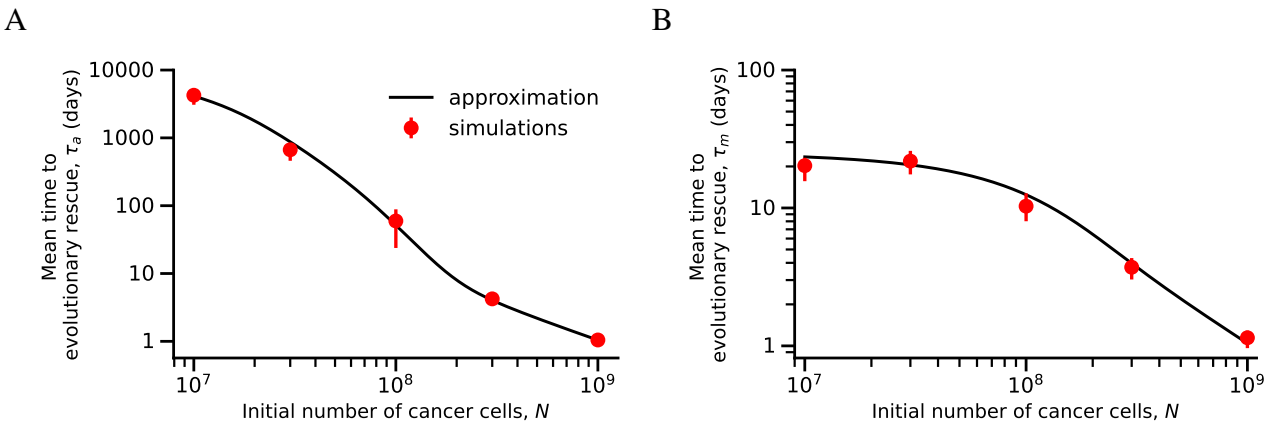

Figure S2: Evolutionary rescue time. Shown is the mean time for appearance of a resistance mutation the leads to evolutionary rescue (A) with aneuploidy ($u > 0$) and (B) without aneuploidy ($u = 0$). Our inhomogeneous Poisson-process approximations (solid black lines, right: eq. (C2), left: eq. (C7)) is in agreement with simulation results (red markers with 95% quantile intervals obtained with bootstrapping, see see Appendix G). Parameters: $\lambda_w = 0.1, \lambda_m = 0.0899, \lambda_m = 0.1, \mu_w = 0.14, \mu_a = 0.09, \mu_m = 0.09, u = 10^{-2}, v = 10^{-7}$.

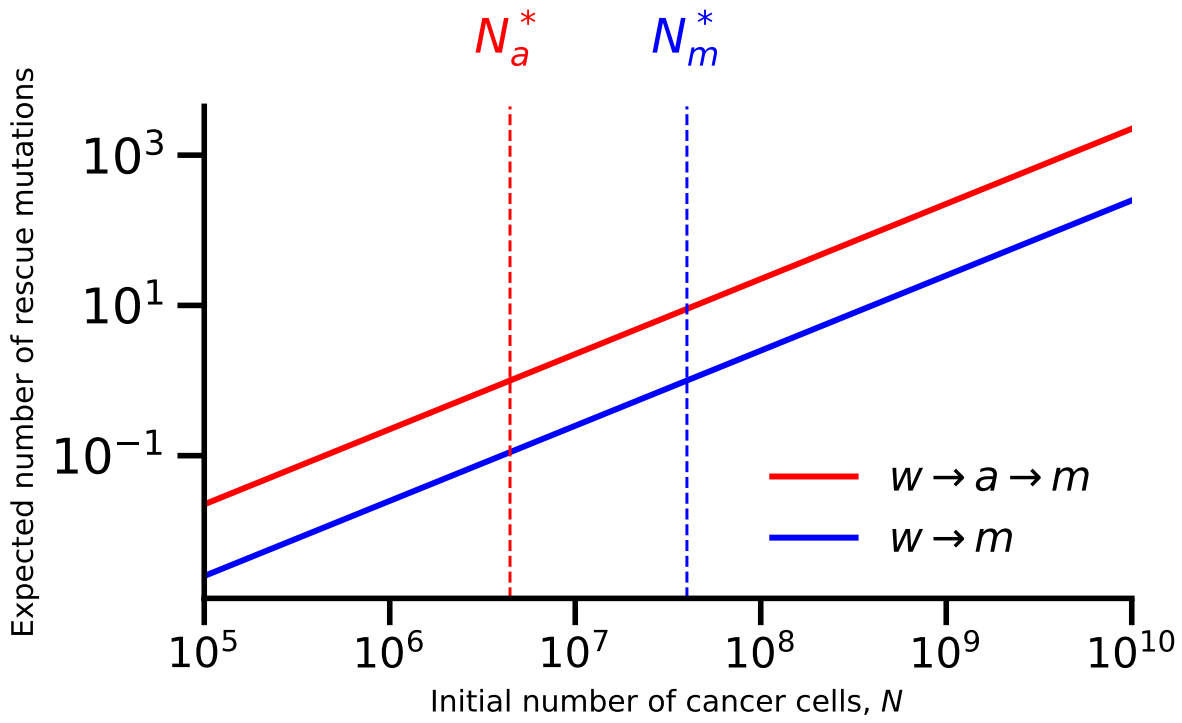

Figure S3: Aneuploidy increases the number of mutations which rescue the tumor. Shown is the expected number of mutation, which will rescue the cancer cell population, produced through the evolutionary trajectory $wildtype \to mutant$ (blue line, eq. (C6)) or through the trajectory $wildtype \to aneuploid \to mutant$ (red line, eq. (C5)). Dashed vertical red line represents the threshold tumor size above which evolutionary rescue is very likely through aneuploidy eq. (4) and the dashed vertical blue line represents the threshold tumor size above which evolutionary rescue is very likely through direct mutation eq. (3). Parameters: $\lambda_w = 0.1, \lambda_m = 0.0899, \lambda_m = 0.1, \mu_w = 0.14, \mu_a = 0.09, \mu_m = 0.09, u = 10^{-2}, v = 10^{-7}$.

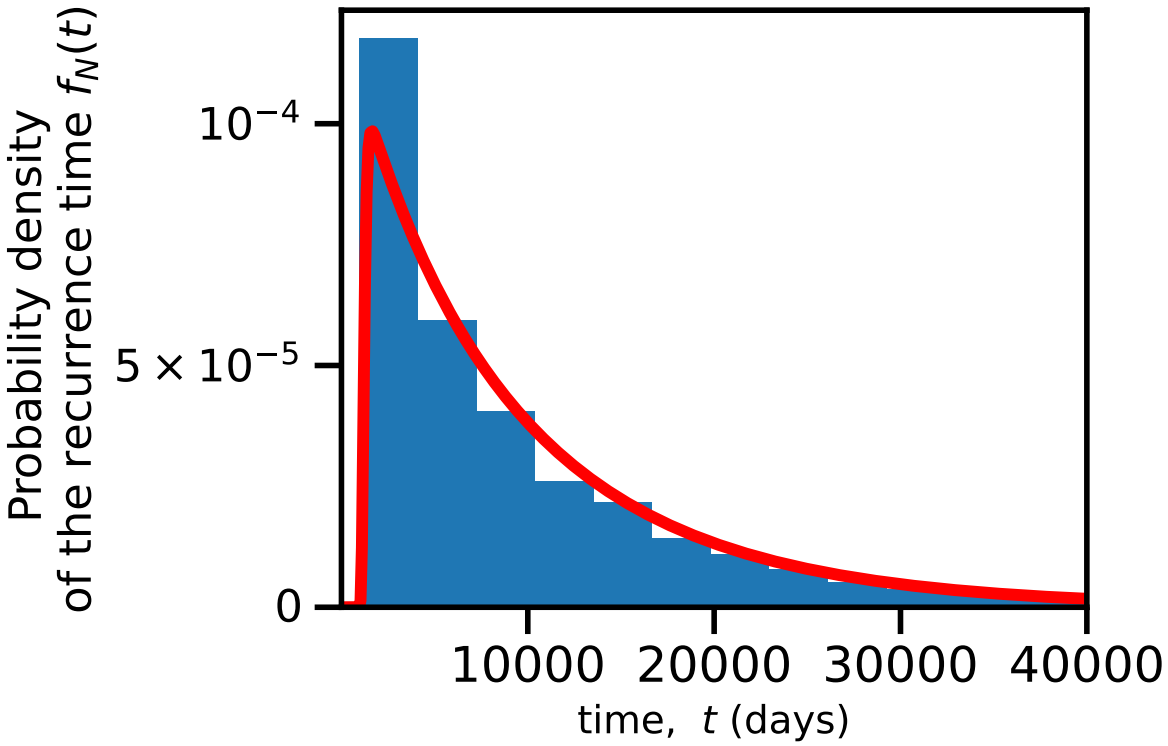

Figure S4: Distribution of the recurrence time. Shown is the distribution of the time for the mutant cell population to reach size N, where N is the initial number of cancer cells. The red line is analytic result eq. (F3) overlaid over the histogram of simulations. Parameters: $N = 10^6, \lambda_w = 0.1, \lambda_a = 0.0899, \lambda_m = 0.1, \mu_w = 0.14, \mu_a = 0.09, \mu_m = 0.09, u = 10^{-2}, v = 10^{-7}$.

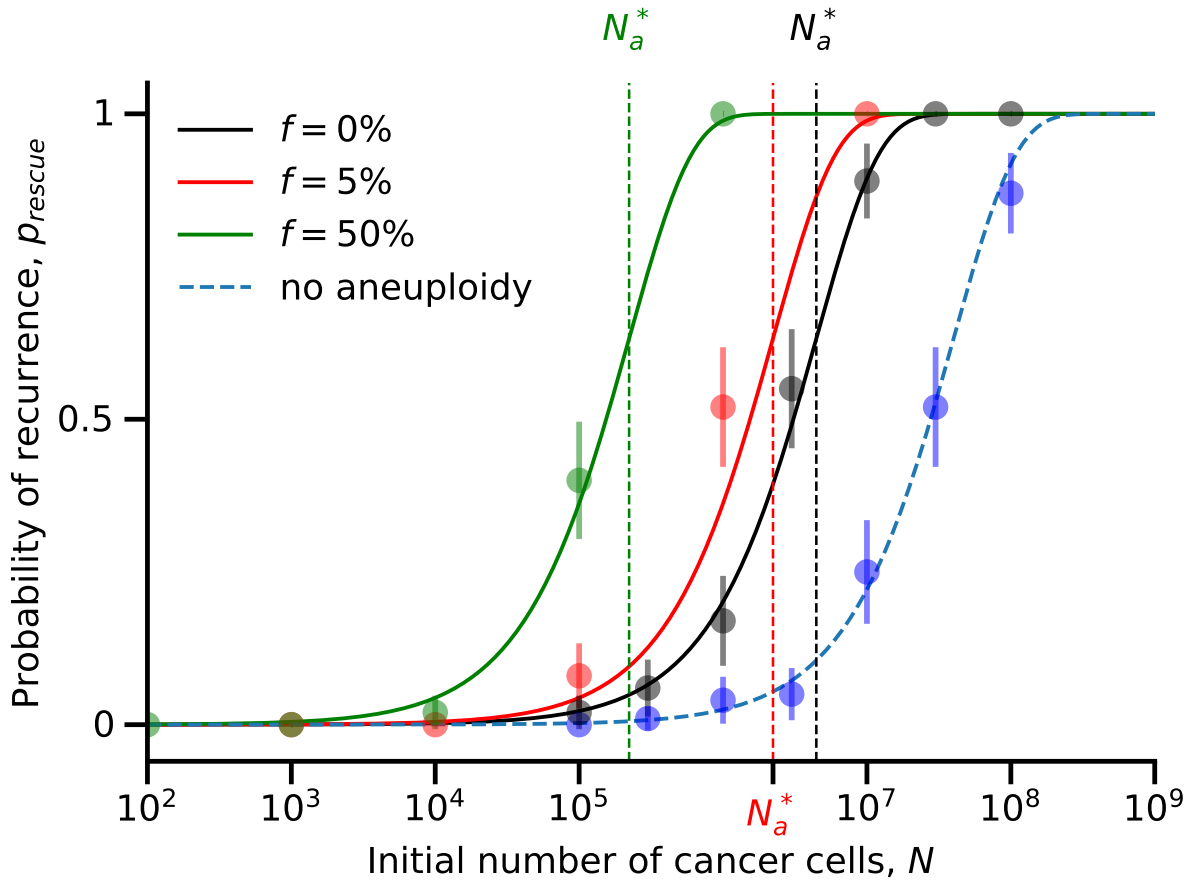

Figure S5: The probability of evolutionary rescue (i.e., the probability that the population does not go to extinction), p_{rescue}, as a function of the initial tumor size, N. Dashed vertical line shows the threshold tumor size, above which the probability is very high. Blue dashed line represents the probability of evolutionary rescue as a function of N without aneuploidy ($u = 0$). The black line represents the scenario where a fraction $f = 0\%$ of the initial tumor is aneuploid, the red line represents the scenario with $f = 5\%$ and the green line represents the scenario with $f = 50\%$. The dots represent simulation results and the error bars represent 95% confidence intervals ($p \pm 1.96\sqrt{p\left(1-p\right)/n}$ where p is the fraction of simulations in which the tumor has adapted to the stress and $n = 100$ is the number of simulations). Parameters: $\lambda_w = 0.1, \lambda_a = 0.0899, \lambda_m = 0.1, \mu_w = 0.14, \mu_a = 0.09, \mu_a = 0.09, \mu_m = 0.09, u = 10^{-2}, v = 10^{-7}$.

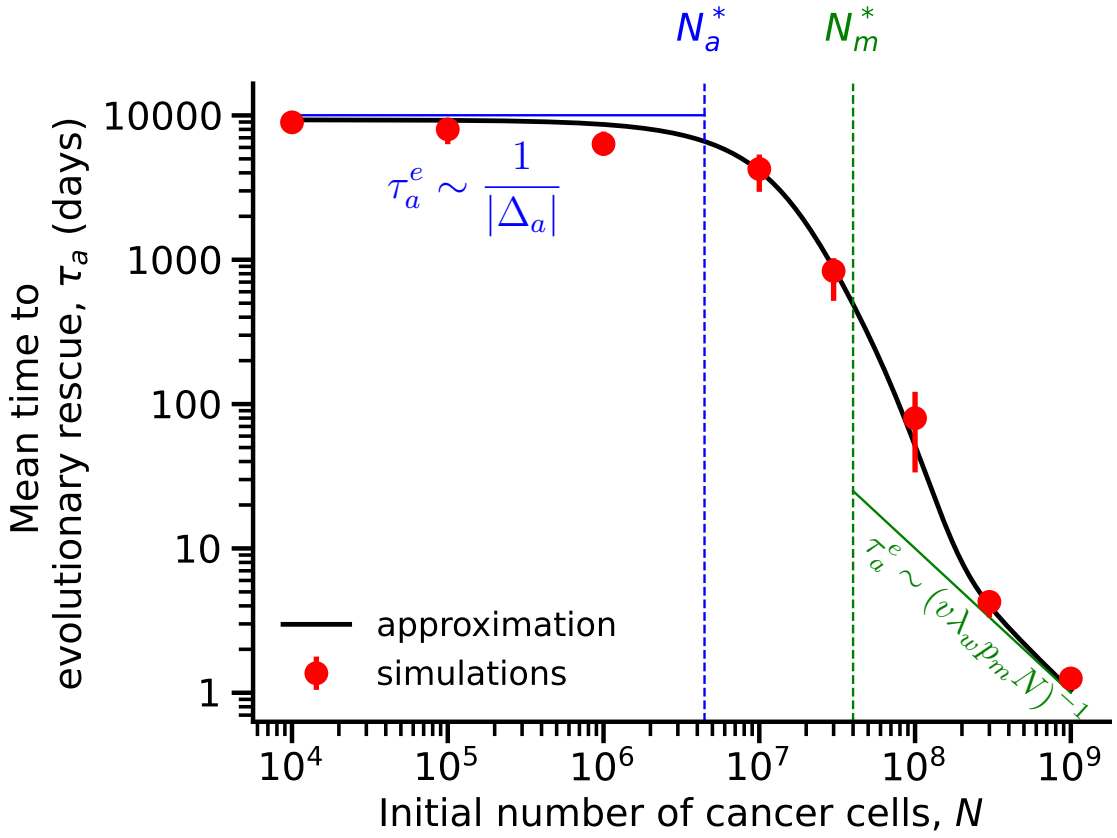

Figure S6: Shown is the mean time for appearance of a resistance mutation the leads to evolutionary rescue with aneuploidy ($u > 0$). Our inhomogeneous Poisson-process approximations (solid black lines, right: eq. (C7)) is in agreement with simulation results (red markers with 95% confidence intervals obtained with bootstrapping, see Appendix G). Dashed vertical blue line represents the threshold tumor size above which evolutionary rescue is very likely through aneuploidy eq. (4) and the dashed vertical green line represents the threshold tumor size above which evolutionary rescue is very likely through direct mutation eq. (3). Solid lines represents the approximations eq. (8) ($N < N_a^*$ blue line and $N > N_m^*$ green line). Parameters: $\lambda_w = 0.1, \lambda_m = 0.0899, \lambda_m = 0.1, \mu_w = 0.14, \mu_a = 0.09, \mu_m = 0.09, u = 10^{-2}, v = 10^{-7}$.

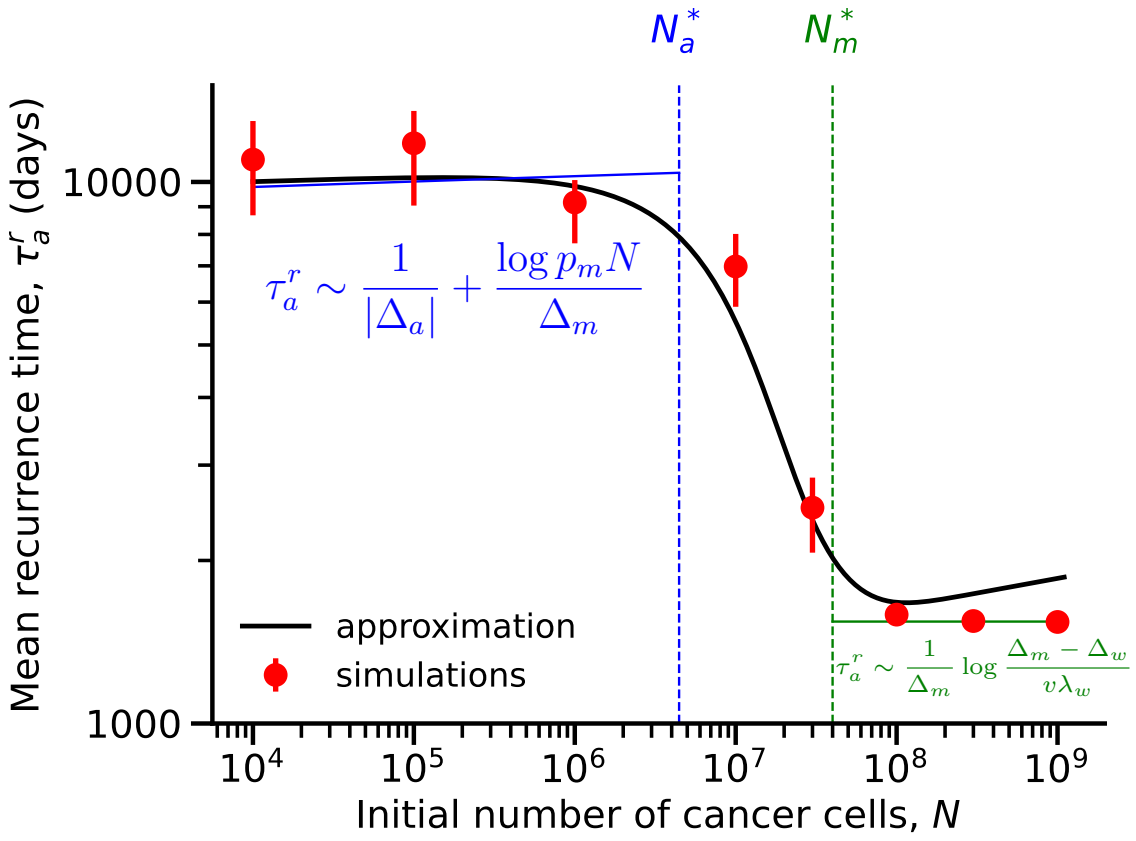

Figure S7: The mean time for the mutant cell population to reach size N, where N is the initial number of cancer cells. Our inhomogeneous Poisson-process approximation (solid black line, eq. (D1)) is in agreement with simulation results (red markers with 95% confidence intervals obtained with bootstrapping, see Appendix G) for small and intermediate values of N. Dashed vertical blue line represents the threshold tumor size above which evolutionary rescue is very likely through aneuploidy eq. (4) and the dashed vertical green line represents the threshold tumor size above which evolutionary rescue is very likely through direct mutation eq. (3). Solid lines represents the approximations eq. (9) ($N < N_a^*$ blue line and $N > N_m^*$ green line). The simulations converge to eq. (D4) (green line) for large values of $N \gg N_m^*$. Parameters: $\lambda_w = 0.1, \lambda_a = 0.0899, \lambda_m = 0.1, \mu_w = 0.14, \mu_a = 0.09, \mu_m = 0.09, u = 10^{-2}, v = 10^{-7}$.

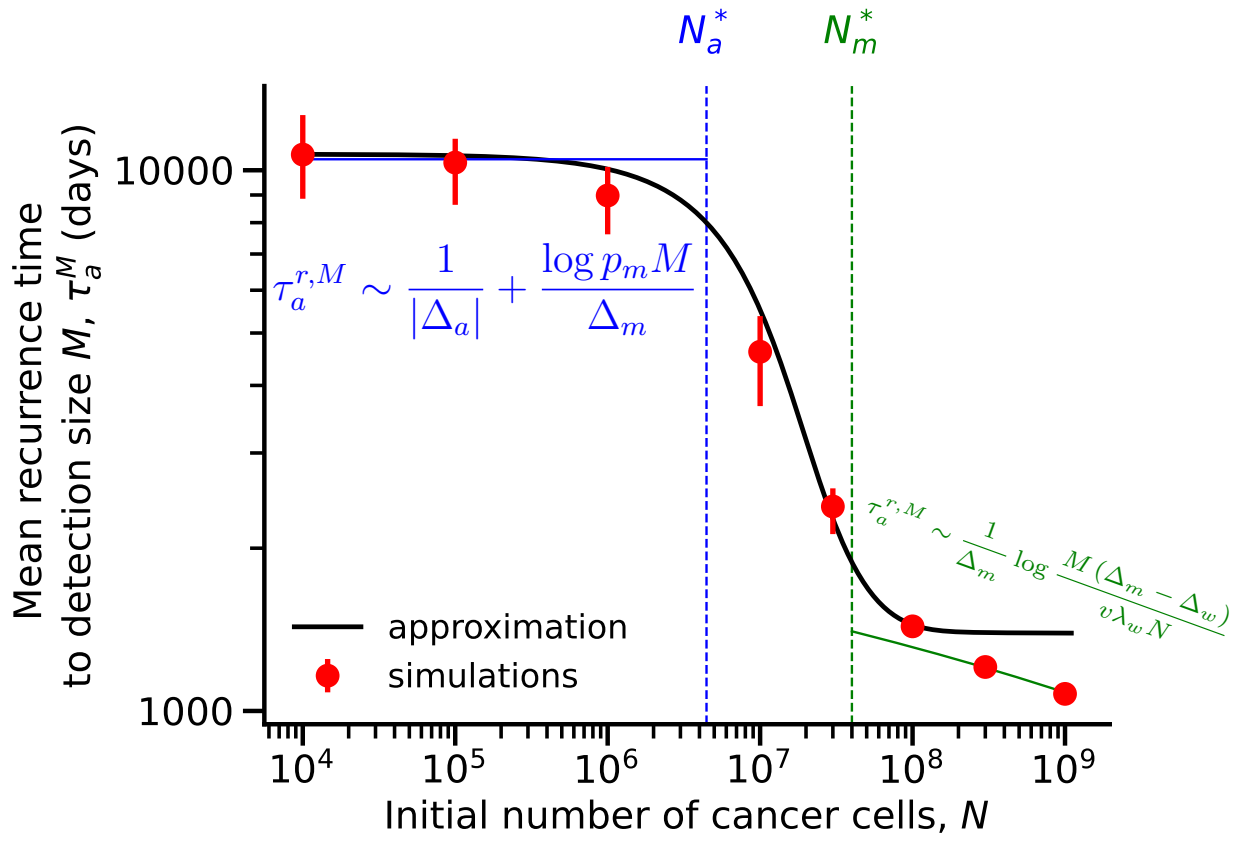

Figure S8: The mean time for the mutant cell population to reach size M, where M is the tumor detection size. Our inhomogeneous Poisson-process approximation (solid black line, eq. (D5)) is in agreement with simulation results (red markers with 95% confidence intervals obtained with bootstrapping, see Appendix G) for small and intermediate values of N. Dashed vertical blue line represents the threshold tumor size above which evolutionary rescue is very likely through aneuploidy eq. (4) and the dashed vertical green line represents the threshold tumor size above which evolutionary rescue is very likely through direct mutation eq. (3). Solid blue line represents the approximation eq. (D5) with τ_a from eq. (8) for $N < N_a^*$ and the solid green line represents the approximation eq. (D6) for $N > N_m^*$. The simulations converge to eq. (D6) (green line) for large values of $N \gg N_m^*$. Parameters: $\lambda_w = 0.1, \lambda_a = 0.0899, \lambda_m = 0.1, \mu_w = 0.14, \mu_a = 0.09, \mu_m = 0.09, u = 10^{-2}, v = 10^{-7}, M = 10^7$.

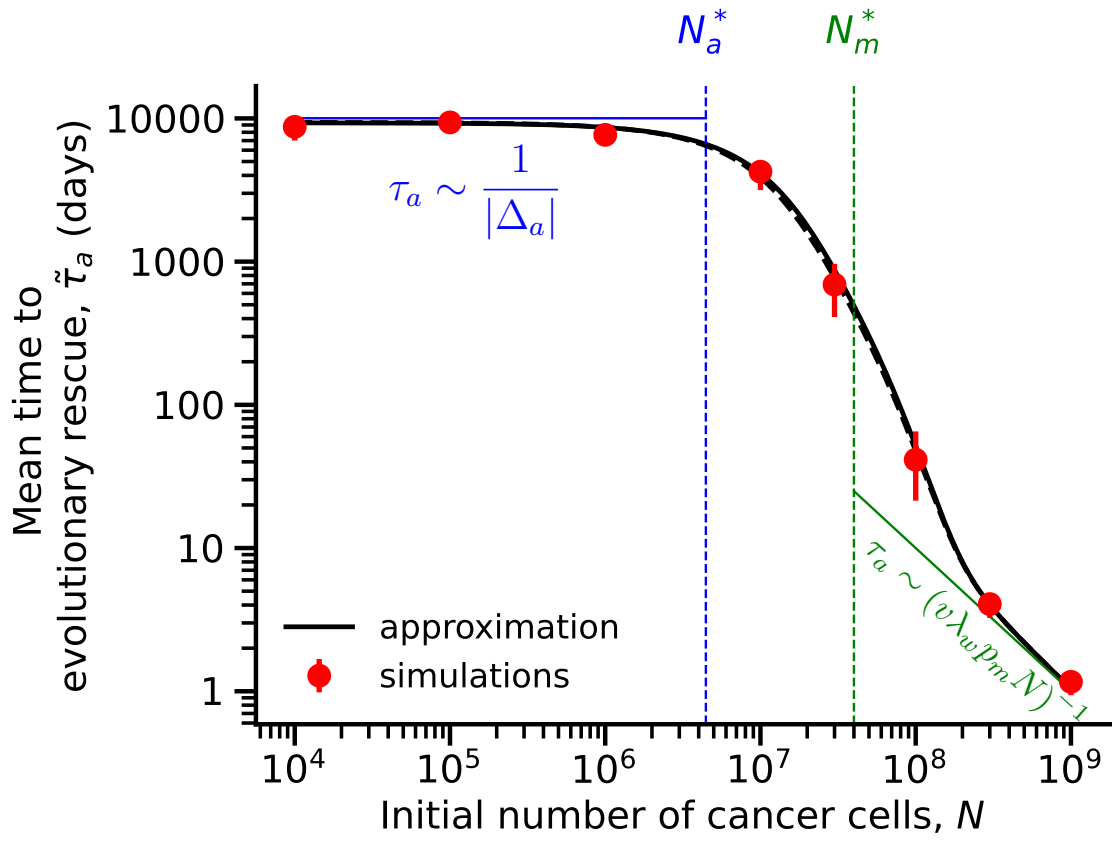

Figure S9: Shown is the mean time for appearance of a resistance mutation the leads to evolutionary rescue with aneuploidy ($u > 0$). Black lines represent our inhomogeneous Poisson-process approximations (solid black line, eq. (C7); dashed black line eq. (C10)). Dashed black line is the inhomogeneous Poisson-process approximation where a fraction f of tumor is aneuploid at the onset of drug therapy which is in agreement with simulation results (red markers with 95% confidence intervals obtained with bootstrapping, see Appendix G). Dashed vertical blue line represents the threshold tumor size above which evolutionary rescue is very likely through aneuploidy eq. (4) and the dashed vertical green line represents the threshold tumor size above which evolutionary rescue is very likely through direct mutation eq. (3). Solid lines represents the approximations eq. (8) ($N < N_a^*$ blue line and $N > N_m^*$ green line). Parameters: $\lambda_w = 0.1, \lambda_m = 0.0899, \lambda_m = 0.1, \mu_w = 0.14, \mu_a = 0.09, \mu_m = 0.09, u = 10^{-2}, v = 10^{-7}, f = 0.284\%$.